

# All You Need Is Hashing: Defending Against Data Reconstruction Attack in Vertical Federated Learning

Pengyu Qiu, Xuhong Zhang, Shouling Ji, Yuwen Pu, Ting Wang

**Abstract**—Vertical federated learning is a trending solution for multi-party collaboration in training machine learning models. Industrial frameworks adopt secure multi-party computation methods such as homomorphic encryption to guarantee data security and privacy. However, a line of work has revealed that there are still leakage risks in VFL. The leakage is caused by the correlation between the intermediate representations and the raw data. Due to the powerful approximation ability of deep neural networks, an adversary can capture the correlation precisely and reconstruct the data.

To deal with the threat of the data reconstruction attack, we propose a hashing-based VFL framework, called *HashVFL*, to cut off the reversibility directly. The one-way nature of hashing allows our framework to block all attempts to recover data from hash codes. However, integrating hashing also brings some challenges, e.g., the loss of information. This paper proposes and addresses three challenges to integrating hashing: learnability, bit balance, and consistency.

Experimental results demonstrate *HashVFL*'s efficiency in keeping the main task's performance and defending against data reconstruction attacks. Furthermore, we also analyze its potential value in detecting abnormal inputs. In addition, we conduct extensive experiments to prove *HashVFL*'s generalization in various settings.

In summary, *HashVFL* provides a new perspective on protecting multi-party's data security and privacy in VFL. We hope our study can attract more researchers to expand the application domains of *HashVFL*.

## I. INTRODUCTION

Recent decades have witnessed the rapid development of machine learning algorithms [1]–[3], especially the deep neural networks (DNNs) [3]–[7]. DNNs have been used in finance [8], [9], biomedicine [4], [10], and even the military [11], [12]. These areas are quite sensitive to data security and privacy. Laws and regulations, e.g., GDPR [13] and CCPA [14], also impose strict restrictions on the flow of data in these areas. Therefore, an apparent contradiction between the model's massive demand for data and the restricted flow of data arises.

P. Qiu, S. Ji, Y. Pu are with the College of Computer Science and Technology at Zhejiang University, Hangzhou, Zhejiang, 310027, China. E-mail: {*qiupys, sji, yw.pu*}@zju.edu.cn

X. Zhang is with the School of Software Technology at Zhejiang University, Ningbo, Zhejiang, 315048, China. E-mail: zhangxuhong@zju.edu.cn

T. Wang is with the College of Information Science and Technology at Pennsylvania State University, State College, PA, 16801, United States. E-mail: inbox.ting@gmail.com

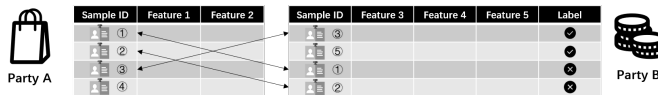


Fig. 1. An example illustration of VFL. Party A is an e-commerce company holding features 1 and 2, and Party B is a bank possessing features 3, 4, 5 and the label. They collaborate to train a model predicting if a loan application should be approved.

Vertical federated learning (VFL) [15]–[18], a trending paradigm, solves one of these dilemmas where companies share the same user group but with different features. Figure 1 shows a typical case in VFL. A bank that wants to improve its model of predicting whether a loan application should be approved may ask an e-commerce company for help to enrich its users' information. In such a situation, each party in VFL will not directly send one user's features but upload its extracted information, i.e., intermediate calculations of the user's features by a bottom model, to a neutral party for aggregation and further computation. Hence, the raw data will not leave the local, and the main challenge becomes to protect the intermediate calculations. Current frameworks of VFL adopt secure multi-party computation (SMC) methods such as homomorphic encryption (HE) [19], [20] to provide data privacy and security guarantee. Specifically, HE enables calculation to be performed in an encrypted environment.

However, a line of work [21]–[24] has revealed that these mechanisms are insufficient. Specifically, when given a sample's posteriors and the VFL model's parameters, an adversary can reconstruct a target party's intermediate calculations and even the raw data. The key to the success of these data reconstruction attacks is the powerful capability of DNNs in modeling the correlation between the intermediate calculations and the raw inputs. For example, generative adversarial networks (GANs) [25], [26] and diffusion models [27], [28], all have achieved astonishing performance in data reconstruction.

Recently, researchers have investigated several ways [29], [30] to defend against the data reconstruction attack in VFL, including expanding the correlation distance between the input and the corresponding activations. These methods do reduce information leakage, but not completely. They still leave the risk of the reconstruction attack if an adversary knows the model and a target sample's output [31].

To cut off the reversibility, we propose a hashing-based VFL framework called *HashVFL*. The one-way nature of

hashing allows our framework to block all attempts to recover intermediate calculations or raw inputs from the hash codes. However, hashing will erase much helpful information and make gradients disappear in models’ training, which means that we may face the problem of degraded performance of the main task. Furthermore, hashing makes it impossible to tell whether a party uploaded a hash code is reliable because we have no other information. A party may use random or wrong hash codes to hinder training for malicious purposes. For example, if the initiator promises to pay for using the party’s data based on the training time, the malicious party may want to extend training for more profit [32]. Moreover, if the party submits the wrong code at inference, this abnormal input may cause misclassification.

Considering the above concerns, we propose three challenges that should be addressed in the design of the hashing-based VFL framework.

- **Learnability.** The challenge is the contradiction between information loss, gradients disappearing, and maintaining the main task’s performance. The key is to find data-dependent hash functions whose gradients are easy to estimate. In this way, the model’s training can continue so that its performance can be guaranteed.

*Our solution:* To achieve the goal, we add a *Sign* function to binarize the intermediate calculations of each party, which is a common practice in hashing [33] and binary neural networks [34]. Then, we adopt *Straight-Through Estimator* [35], [36], which passes the gradient exactly as it is through the *Sign* function in back-propagation to avoid gradient vanishment.

- **Bit balance.** Conventional scenarios that apply hashing, e.g., retrieval, should consider the impact of hash collision, i.e., two different samples have the same hash code. Hence, these methods may keep a long hash code to reduce the probability of hash collision. However, our hashing mechanism aims to minimize information leakage, which requires the length of hash codes to be as short as possible. Furthermore, it is also a good quality if samples of the same category can be mapped to the same hash code for classification. Therefore, we propose bit balance to emphasize how to maximize the use of each bit when the length of the hash code is limited. Ideally, half of all samples should be mapped to 1/-1 (the value depends on specific hash functions) on one bit.

*Our solution:* Considering the requirement, we find that *Batch Normalization* [37] is a suitable solution for this challenge. Batch normalization can make each dimension of the intermediate calculation of a batch of samples obey the standard normal distribution and dynamically learn the mean and variance suitable for the entire training set. Hence, it can address the effectiveness problem of the bit without hurting the main task’s performance.

- **Consistency.** Assuming that all parties involved in VFL are benign is unrealistic. Therefore, a safe training scheme needs to pre-set this malicious situation to occur.

A natural constraint is that the hash codes of a sample should be consistent across different parties. In this way, we can notice abnormal inputs if the constraint is not satisfied by calculating the difference between these parties’ hash codes. However, one problem is that if we calculate the difference between the parties pair by pair, the computational overhead will be unbearable when there are many parties.

*Our solution:* We pre-define a set of binary codes for each class [38] to solve the dilemma. In this way, each party only needs to compare their hash codes with these binary codes. Hence, we can reduce the computation complexity from  $O(N^2)$  to  $O(N)$ , where  $N$  is the number of parties, and support cases where many parties are involved. Moreover, from the derivation in [39], the calculated difference between the sample’s code with the target binary code can also guide the optimization.

Experimental results show that our proposed *HashVFL* keeps the main task’s performance across various data types. Furthermore, in addition to defending against data reconstruction attacks, it can help detect abnormal inputs, which benefits from our address on consistency. We also evaluate *HashVFL*’s ability with various factors, e.g., the number of parties, the length of hash codes, etc. Moreover, we further conduct the ablation study on analyzing the impact of bit balance and consistency on *HashVFL*. The experimental results demonstrate *HashVFL*’s capability of handling these different scenarios.

In summary, our contributions are:

- We propose a new perspective on protecting data security and privacy in VFL. As far as we know, we are the first work that integrates hashing.
- We propose three challenges that should be addressed in the design of the hashing-based VFL framework, i.e., learnability, bit balance, and consistency. We solve them respectively and provide a feasible implementation.
- We present a comprehensive empirical evaluation of *HashVFL* on classification tasks. The results show that our framework is easy to use and supports different model architectures, data types, and multi-party scenarios.
- We also experimentally demonstrate the effectiveness of *HashVFL* in defending against data reconstruction attacks and detecting abnormal inputs. We hope that *HashVFL* can attract more researchers to expand its application domains in practice.

## II. BACKGROUND

This section provides the background information for DNN, VFL, data reconstruction attacks, hashing, and our threat model. Table I summarizes the necessary notations.

### A. Deep Neural Networks

Deep neural networks (DNNs) have been greatly developed in recent decades for their powerful learning ability. Specifically, a DNN  $f$  with parameters  $\theta$  represents a function  $f : \mathcal{X} \rightarrow \mathcal{Y}$ , where  $\mathcal{X}$  denotes the input space and  $\mathcal{Y}$  denotes the corresponding classes. We mainly introduce the application

TABLE I  
SYMBOLS AND NOTATIONS.

Notations	Definition
$P_i, D_i$	the $i$ -th party in VFL, and $P_i$ 's dataset
$\mathcal{U}_i, \mathcal{F}_i$	$D_i$ 's sample/user space and feature space
$f_i, f_{top}$	$P_i$ 's bottom model and the top model
$\theta_i, \theta_{top}$	$f_i$ 's parameters, and $f_{top}$ 's parameters
$\mathbf{x}_i^{(u)}, \mathbf{v}_i^{(u)}, \mathbf{h}_i^{(u)}$	a sample $u$ 's feature vector of $D_i$ , $\mathbf{x}_i^{(u)}$ 's corresponding output from $f_i$ , and the hash code of $\mathbf{v}_i^{(u)}$

of DNNs in classification tasks in this section, and a detailed example is presented as follows.

Given a training set  $D$ , of which each instance  $(\mathbf{x}, y) \in D \subset \mathcal{X} \times \mathcal{Y}$  consists of an input  $\mathbf{x}$  and its label  $y$ , a DNN  $f$  is trained to learn the best parameters  $\theta$  by minimizing a loss value calculated by a function  $\ell$  (usually a cross-entropy loss for classification tasks). The search for the best  $\theta$  can be formulated as:

$$\min_{\theta} \mathbb{E}_{(\mathbf{x}, y) \in D} [\ell(\mathbf{x}, y; \theta)],$$

where  $\mathbb{E}[\cdot]$  denotes the expectation of the loss values on  $D$ .

### B. Vertical Federated Learning

VFL is an emerging paradigm that enables multi-party collaboration to build a machine learning model. Formally, we give the detailed description as follows.

Consider a classification task and a set of  $N$  parties  $\{P_1, P_2, \dots, P_N\}$  with datasets  $\{D_1, D_2, \dots, D_N\}$ .  $D_i$  can further be described as  $D_i = (\mathcal{U}_i, \mathcal{F}_i)$ , where  $\mathcal{U}_i$  denotes the sample/user space and  $\mathcal{F}_i$  denotes the feature space. Before training, parties have to prepare an overlapped sample space  $\mathcal{U}$ , which is the intersection of the above sample space, i.e.,  $\mathcal{U} = \bigcap_{i=1}^N \mathcal{U}_i$ . Then, for samples in  $\mathcal{U}$ , their features in different  $\mathcal{F}_i$  will be align according to their new index in  $\mathcal{U}$ .

After the preparation of training set,  $P_i$  trains its bottom model,  $f_i$ . Let  $\mathbf{x}_i^{(u)}$  denotes the feature vector (raw input) of the sample  $u$  from  $\mathcal{F}_i$ . The function of  $f_i$  is to map it into a  $\tilde{d}$ -dimensional latent space, i.e.,  $f_i(\mathbf{x}_i; \theta_i) : \mathbb{R}^{d_i} \rightarrow \mathbb{R}^{\tilde{d}}$ , where  $\theta$  denotes the model's parameters, and  $d_i$  refers to the size of  $\mathbf{x}_i$ 's dimension. We use  $\mathbf{v}_i^{(u)}$  to represent  $u$ 's output of  $f_i$ .

Then,  $\mathbf{v}_i^{(u)}$  will be sent to a neutral third party's server for aggregation and further calculation. Specifically, let  $\mathbf{v}_{cat}^{(u)} = [\mathbf{v}_1^{(u)}, \mathbf{v}_2^{(u)}, \dots, \mathbf{v}_N^{(u)}]$  denote the concatenated vector of the sample  $u$  and  $f_{top}$  denote the top model deployed at the server.  $f_{top}$  is supposed to learn a mapping from  $\mathbf{v}_{cat}^{(u)}$  to  $\mathbf{v}_{top}^{(u)}$ , where  $\mathbf{v}_{top}^{(u)}$  is also the posterior for classification. Formally,  $f_{top}$  can be presented as  $f_{top}(\mathbf{v}_{cat}; \theta_{top}) : \mathbb{R}^{N \times \tilde{d}} \rightarrow \mathbb{R}^C$ , where  $C$  denote the number of classes.

Finally,  $\mathbf{v}_{top}^{(u)}$  will be sent to the party who owns the label. Then, the party calculates the loss, e.g., cross-entropy loss, and the corresponding gradients. Using the chain rule, each model's parameters can be updated by passing the gradients. The above process can be formulated as:

$$\min_{\{\theta_i\}_{i=1}^N, \theta_{top}} \mathbb{E}_{u \in \mathcal{U}} [\ell(\mathbf{x}_1^{(u)}, \mathbf{x}_2^{(u)}, \dots, \mathbf{x}_N^{(u)}, y; \{\theta_i\}_{i=1}^N, \theta_{top})],$$

where  $\ell$  denotes the loss function, and  $y$  is the label of  $u$ .

During training, intermediate calculations and gradients are transmitted, which are sensitive. Existing frameworks, e.g., FATE [40], PySyft [41], TF Encrypted [42], and CrypTen [43], apply HE [44] to provide privacy guarantee. In a nutshell, HE enables vectors to be added and multiplied with encryption.

### C. Data Reconstruction Attack

In DNN's development, one criticism is endless, i.e., the model will leak information and thus violate the privacy of the user whose data is being collected. Images, widely used in computer vision tasks, are the hardest hit area.

In [45], Zhu et al. showed that the data could be reconstructed from the leaked gradients. Specifically, they let the generated sample's gradients approximate the target sample's gradients as close as possible and achieved a good performance. Formally, the attack can be formulated as follows:

$$\tilde{\mathbf{x}}^*, \tilde{y}^* = \arg \min_{\tilde{\mathbf{x}}, \tilde{y}} \left\| \frac{\partial \ell(f(\tilde{\mathbf{x}}, \theta), \tilde{y})}{\partial \theta} - \nabla \theta \right\|^2,$$

where  $\tilde{\mathbf{x}}^*$ ,  $\tilde{y}^*$  are reconstructed sample and its inferred label;  $\ell(\cdot)$  denotes the loss function;  $f, \theta$  denotes the model and its parameters; and  $\nabla \theta$  is the target sample's gradients.

In [46], Pasquini et al. showed that an adversary could reconstruct the target image with knowledge of the model and the target image's posteriors under split learning scenarios. Ergodan et al. [47] showed that the knowledge can further be relaxed to the model structure's copy and the target sample's intermediate calculations. In [31], He et al. unified model stealing and data reconstruction attack. The attack can be formulated as follows:

$$\begin{cases} \tilde{\mathbf{x}}^* = \arg \min_{\tilde{\mathbf{x}}} \ell(f_{\tilde{\theta}}(\tilde{\mathbf{x}}), f_{\theta}(\mathbf{x})) + L(\tilde{\mathbf{x}}) \\ \tilde{\theta}^* = \arg \min_{\tilde{\theta}} \ell(f_{\tilde{\theta}}(\tilde{\mathbf{x}}), f_{\theta}(\mathbf{x})), \end{cases}$$

where  $\tilde{\mathbf{x}}^*$  is the reconstructed sample;  $f, \theta$  denotes the model and its parameters;  $\tilde{\theta}^*$  is the approximated parameters;  $\ell(\cdot, \cdot)$  measures the distance between two terms; and  $L(\tilde{\mathbf{x}})$  denotes the penalty function of  $\tilde{\mathbf{x}}$  to guide the generation. For example, in [31], they used the Total Variation term [48] to smooth the noise. Moreover, the optimization was alternated between samples and parameters to achieve the best results.

In [21], Luo et al. revealed that the encryption mechanism in VFL cannot prevent the adversary from reconstructing the data by a generative adversarial network. Weng et al. [22] also verified the conclusion across more machine learning algorithms. Moreover, in [23], Qiu et al. also showed that the reconstructed intermediate calculations could reflect the topology information used in graph neural networks.

In summary, side channel information, such as gradients, and intermediate calculations, can leak what it connects with due to the powerful approximation ability of DNNs.

### D. Hashing

Conventional hash functions are data-independent, meaning their design does not retain data information. For example, MD5 hashing [49] takes an input message of arbitrary length

and produces an output 128-bit ‘‘fingerprint’’ or ‘‘message digest’’ through groups and other math operations.

However, the search for complex data, such as similar image retrieval, product recommendation, etc., has spawned a class of data-dependent hashing methods. For example, Locality-Sensitive Hashing (LSH) [50] is widely used in approximate nearest neighbor (ANN) searching. Specifically, for two samples  $u$  and  $v$ , LSH requires that their hash codes should have the property:

$$Pr[h(\mathbf{x}^{(u)}) = h(\mathbf{x}^{(v)})] : \begin{cases} \geq p_1 & \text{if } d(\mathbf{x}^{(u)}, \mathbf{x}^{(v)}) \leq d_1 \\ \leq p_2 & \text{else } d(\mathbf{x}^{(u)}, \mathbf{x}^{(v)}) \geq d_2, \end{cases}$$

where  $\mathbf{x}^{(u)}$  denotes the sample  $u$ ’s feature vector,  $h(\cdot)$  is the hash function,  $d(\cdot)$  is the distance calculation function,  $p_1, p_2$ , and  $d_1, d_2$  are specific values of probability and distance.

The property means that for two samples’ feature vectors, if their distance is less than  $d_1$ , their hash code should at least have the probability  $p_1$  to have the same value; on the contrary, if it is less than  $d_2$ , the probability of their hash codes are same should not beyond  $p_2$ .

Recently, a line of work [33], [51]–[53] has found the powerful capability of DNNs in keeping the property of data-dependent hashing for approximate nearest neighbour searching. The idea is to use DNNs to extract abstract presentations and then binarize the presentations. In this way, they could maintain the samples’ correlation and keep the retrieval effectiveness. Our *HashVFL* also refers to these works to address learnability.

### E. Threat Model

We assume that the server and all parties are honest-but-curious [54] adversaries, i.e., they will follow all requirements as specified in VFL but are curious about the intermediate calculation and raw data located on the target party. Moreover, we assume that the adversary knows each other’s bottom model and samples’ hash codes, i.e., only the local data of each party is strictly confidential.

## III. METHODOLOGY

This section provides the framework of *HashVFL* and the implementation details of each component.

### A. Overview

Figure 2 shows the overview pipeline of *HashVFL*. We present the details as follows.

First, each party,  $P_i$ , where  $i \in \{1, 2, \dots, N\}$  and  $N$  is the number of parties, prepares the training dataset  $D_i = (\mathcal{U}, \mathcal{F}_i)$ . Then,  $P_i$  chooses a specific model,  $f_i$ , for extracting information from the raw data,  $\mathbf{x}_i$ . For example, if  $D_i$  is an image dataset, ResNet [55] and VGG [56] are feasible candidates, which are popular model architectures for image classification. We use  $\mathbf{x}_i$  to denote a sample’s feature vector at  $D_i$ , and  $\mathbf{X}_i$  to denote a batch of samples’ feature vectors.

Next, the outputs of  $\mathbf{X}_i$  from  $f_i$ , i.e.,  $\mathbf{V}_i$ , go through a Batch Normalizing transform (BN) layer, which is mandatory. The transformed outputs,  $\tilde{\mathbf{V}}_i$ , now achieve a balance at each

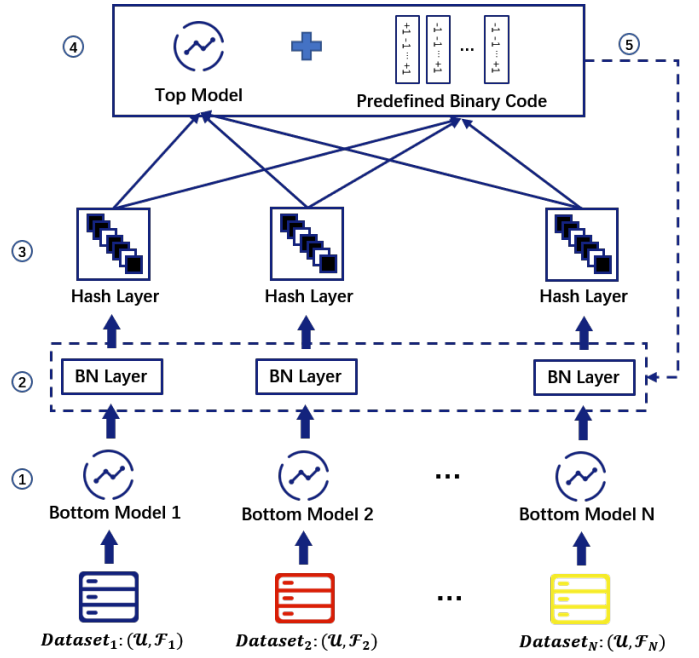


Fig. 2. Overview of *HashVFL*. 1) Each party uses their bottom model to extract abstractions from local data. 2) A batch of abstractions must go through the batch\_norm layer for normalization. 3) Normalized abstractions obtained from 2) are binarized by the hash layer, and then uploaded to the server. 4) The server uses the top model to calculate classification loss and calculates the distance between these codes and their target pre-defined binary codes. 5) The server computes the gradients, and send them back to each party. Since we use STE, the gradients will directly pass through the hash layer, and the updates begin from the batch\_norm layer.

dimension, thus satisfying our ‘bit balance’ requirement. Then, these balanced outputs have to be binarized by a hash layer. We use  $\mathbf{H}_i$  to denote the hash codes.

Finally,  $\mathbf{H}_i$  are concatenated at the server side, i.e.,  $\mathbf{H} = [\mathbf{H}_1, \dots, \mathbf{H}_N]$ . The top model calculates the classification loss, usually cross-entropy loss, of  $\mathbf{H}$ . Meanwhile,  $\mathbf{H}_i$  is also compared to pre-defined binary codes  $\mathbf{o} \in \{-1, +1\}^{C \times \tilde{d}}$ , where  $C$  is the number of classes and  $\tilde{d}$  is the size of the hash code, for the consistency requirement. Specifically, we calculate the distance between  $\mathbf{h}_i^{(u)} \in \mathbf{H}_i$  and its target binary code  $\mathbf{o}_y$ , where  $u$  denotes a sample in the batch with label  $y$ ,  $\mathbf{h}_i^{(u)}$  refers to  $u$ ’s hash code, and  $\mathbf{o}_y$  denotes the class  $y$ ’s corresponding code.

During the back-propagation process, the gradients are passed as they are through the hash layer. Therefore, only BN layers’ parameters and  $\theta_i$  need to be updated.

The pipeline is the same as the above description at inference time but without the back-propagation process. Algorithm 1 describes the mainframe of *HashVFL* in training.

In the following, we present the details of our implementation about the BN layer, the Hash layer, and the design of pre-defined binary codes.

### B. BN Layer

Batch Normalization (BN) was first proposed by Sergey et al. [37] to solve the problem of *Internal Covariate Shift*. That

---

**Algorithm 1** Mainframe of *HashVFL* in the training.

---

**Input:**  $\{D_i, f_i\}_{i=1}^N, f_{top}$ , pre-defined binary codes  $\mathbf{o}$ , training epochs  $Epochs$

**Output:**  $\{f_i\}_{i=1}^N, f_{top}$  for inference

```
1: for  $i \leq Epochs$  do
2:   for each batch  $(\mathbf{X}, \mathbf{Y})$  do
3:     During forward process:
4:     for At each  $P_i$  do
5:        $\mathbf{V}_i \leftarrow f_i(\mathbf{X}_i)$ 
6:        $\tilde{\mathbf{V}}_i \leftarrow BN(\mathbf{V}_i)$ 
7:        $\mathbf{H}_i \leftarrow Sign(\tilde{\mathbf{V}}_i)$ 
8:       Send  $\mathbf{H}_i$  to the server
9:     end for
10:    At the server:
11:     $\mathbf{H} \leftarrow \text{concate}(\{\mathbf{H}_i\}_{i=1}^N)$ 
12:     $Posterior_s \leftarrow f_{top}(\mathbf{H})$ 
13:     $Targets \leftarrow \text{onehot}(\mathbf{Y}) \times \mathbf{o}$ 
14:     $Loss \leftarrow CE(Posterior_s, \mathbf{Y}) + \text{dist}(\mathbf{H}, Targets)$ 
15:    During backward process:
16:    At the server:
17:    for each  $\mathbf{H}_i$  do
18:      Calculate  $\frac{\partial Loss}{\partial \mathbf{H}_i}$ 
19:      Send  $\frac{\partial Loss}{\partial \mathbf{H}_i}$ 
20:    end for
21:    for At each  $P_i$  do
22:       $\frac{\partial Loss}{\partial \tilde{\mathbf{V}}_i} \leftarrow \frac{\partial Loss}{\partial \mathbf{H}_i}$ 
23:      Update the following parameters
24:    end for
25:  end for
26: end for
```

---

is, during neural networks' training, the distribution of activations will shift due to the change in networks' parameters, In this paper, however, we use the design of BN to address our proposed bit balance.

Formally, given a batch of samples  $\mathcal{B} = \{\mathbf{x}^{(1)}, \mathbf{x}^{(2)}, \dots, \mathbf{x}^{(m)}\}$ , where  $m$  denotes the size of the batch, a BN layer first normalizes each  $\mathbf{x}^{(i)}$  with batch mean  $\mu_{\mathcal{B}} : \frac{1}{m} \sum_{i=1}^m \mathbf{x}^{(i)}$  and batch variance  $\sigma_{\mathcal{B}}^2 : \frac{1}{m} \sum_{i=1}^m (\mathbf{x}^{(i)} - \mu_{\mathcal{B}})^2$ , i.e.,  $\bar{\mathbf{x}}^{(i)} : \frac{\mathbf{x}^{(i)} - \mu_{\mathcal{B}}}{\sqrt{\sigma_{\mathcal{B}}^2 + \epsilon}}$ , where  $\bar{\mathbf{x}}^{(i)}$  denotes normalized value, and set  $\epsilon$  to prevent from division by zero. Hence, we have  $\sum_{i=1}^m \bar{\mathbf{x}}^{(i)} = 0$  and  $\frac{1}{m} \sum_{i=1}^m \bar{\mathbf{x}}^{2(i)} = 1$ , if we neglect  $\epsilon$ . In such a way, we can guarantee that in each batch, the samples are evenly assigned positive and negative values on each bit.

However, simply normalizing each input of a layer may change what the layer can represent [37]. Therefore, there are two more parameters  $\gamma$  and  $\beta$  in the BN layer to scale and shift the normalized value:  $\tilde{\mathbf{x}}^{(i)} = \gamma \bar{\mathbf{x}}^{(i)} + \beta$ . This way, *BN* can recover the original activations if that is optimal for training. Furthermore, these two parameters can capture the statistical information of the training dataset, which is helpful for inference.

During inference, for a batch of samples  $\mathcal{B}_{inf}$ , we transform them with  $\tilde{\mathbf{x}} = \frac{\gamma}{\sqrt{Var[\mathbf{x}] + \epsilon}} \bar{\mathbf{x}} + (\beta - \frac{\gamma \mathbb{E}[\mathbf{x}]}{\sqrt{Var[\mathbf{x}] + \epsilon}})$ , where  $\mathbb{E}[\mathbf{x}] =$

$$\mathbb{E}_{\mathcal{B}_{inf}}[\mu_{\mathcal{B}_{inf}}] \text{ and } Var[\mathbf{x}] = \frac{m}{m-1} \mathbb{E}_{\mathcal{B}_{inf}}[\sigma_{\mathcal{B}_{inf}}^2].$$

### C. Hash Layer

Hashing is an NP-hard binary optimization problem [57]. Therefore, a line of work [53] adopts *tanh* or *sigmoid* for approximation, which ensures the differentiability. However, these attempts still leave the risks of leakage in training. Therefore, we use the *Sign* function for binarization, which provides protection from training to inference. Formally, the *Sign* function is defined as follows:

$$h = Sign(v) = \begin{cases} +1 & \text{if } v \geq 0 \\ -1 & \text{otherwise,} \end{cases}$$

where  $h$  is the binary value of the input  $v$ . For vectors, the function operates element-wise.

Then, to solve the vanishment of gradients by using *Sign*, we combine the *Straight-Through Estimator* (STE) in back-propagation. In [35], to solve the challenge of estimating the gradients when stochastic or hard non-linearity neurons are used in neural networks, Bengio et al. proposed four estimators. STE is the most efficient solution as it behaves like the identity function. Specifically, given a vector  $\mathbf{v}$  and its hash code  $\mathbf{h}$ , which is obtained through the *Sign* function, the gradients  $\mathbf{g}$  of  $\mathbf{v}$  can be estimated as:

$$\mathbf{g} = \frac{\partial L}{\partial \mathbf{v}} = \frac{\partial L}{\partial \mathbf{h}} \cdot \frac{\partial \mathbf{h}}{\partial \mathbf{v}} \approx \frac{\partial L}{\partial \mathbf{h}},$$

where  $L$  is the calculated loss of  $\mathbf{v}$ . With such an approximation, the model's training can thus continue.

### D. Generation of Pre-defined Binary Codes

The pre-defined binary codes are used to reduce the computation complexity in keeping the hash codes' consistency. Moreover, they are also important for the classification task.

According to [58], the probability of two vectors  $\mathbf{v}_i$  and  $\mathbf{v}_j$  to have the same hash code under a family of hash functions using random hyperplane techniques is  $1 - \frac{\theta_{ij}}{\pi}$ , where  $\theta_{ij}$  denotes the angle between  $\mathbf{v}_i$  and  $\mathbf{v}_j$ . Therefore, to make the sample's hash codes discriminative for the task, we should let the pre-defined binary codes be as independent of each other as possible, i.e., orthogonal to each other.

To achieve the orthogonality, we follow the practice in [39], i.e., randomly generating the binary codes according to the Bernoulli distribution with  $p = \frac{1}{2}$ , where  $p$  denotes the probability of signing +1 on each bit. The derivation of  $p$  is as follows.

First, for two randomly generated binary codes  $\mathbf{o}_1$  and  $\mathbf{o}_2$  with size  $n$ , we have  $Pr(\cos(\mathbf{o}_1, \mathbf{o}_2) = 0) = Pr(\sum_{i=1}^n o_{1i} \cdot o_{2i} = 0)$ . Since  $o_{1i}$  and  $o_{2i}$  both obey the Bernoulli distribution with  $p$ , the probability  $q$  of that  $o_{1i}$  and  $o_{2i}$  have the same value is  $p^2 + (1-p)^2$ .

Then,  $\sum_{i=1}^n o_{1i} \cdot o_{2i}$  becomes the binomial distribution with  $q$ , i.e.,  $n$  consecutive Bernoulli trials. Hence,  $Pr(\sum_{i=1}^n o_{1i} \cdot o_{2i} = 0) = \binom{n}{\frac{n}{2}} q^{\frac{n}{2}} (1-q)^{\frac{n}{2}}$ . For a specific  $n$ ,  $\binom{n}{\frac{n}{2}}$  is a constant. With inequality  $q(1-q) \leq (\frac{q+(1-q)}{2})^2$ , where the equal sign is obtained when  $q = 1-q$ , we have  $q = \frac{1}{2}$  to maximize

$Pr(\cos(\mathbf{o}_1, \mathbf{o}_2) = 0)$ . Therefore,  $p^2 + (1-p)^2 = \frac{1}{2}$ , where we finally prove that  $p = \frac{1}{2}$  is the best.

### E. Metrics of Distance

Hamming distance [59] is commonly used in binary codes' distance calculation, while in this paper, we mainly discuss with the cosine similarity. The reason is that they are literally equal for binary codes [39].

For example, given a sample's hash code  $\mathbf{h}$  and its corresponding target binary code  $\mathbf{o}$ , the hamming distance between them is:  $H(\mathbf{h}, \mathbf{o}) = \frac{\tilde{d} - \mathbf{h}^T \mathbf{o}}{2}$ , where  $H(\cdot)$  is the hamming distance calculation function and  $\tilde{d}$  is the length of codes.

Then, since  $\mathbf{h}^T \mathbf{o} = \|\mathbf{h}\| \|\mathbf{o}\| \cos\theta$ , where  $\|\cdot\|$  is the Euclidean norm and  $\theta$  is the angle between  $\mathbf{h}$  and  $\mathbf{o}$ , and both  $\|\mathbf{h}\|$  and  $\|\mathbf{o}\|$  equal to  $\sqrt{\tilde{d}}$ , we have:  $H(\mathbf{h}, \mathbf{o}) = \frac{\tilde{d} - \tilde{d} \cos\theta}{2} = \frac{\tilde{d}}{2}(1 - \cos\theta)$ . Therefore, minimizing the hamming distance equals to minimizing the angle between the two binary codes, which also means to maximize the cosine similarity between them.

## IV. EXPERIMENTAL SETUP

We set up a *HashVFL* framework as depicted in Figure 2. In this paper, we primarily consider the two-party VFL, following [21]–[24]. It is reasonable as in industry, the communication cost and the computation overhead will increase rapidly with the increase of the number of parties. Therefore, two-party VFL is now the most popular scenario in the real-world [17]. However, we also evaluate the impact of the number of parties in Section VI-A.

In this section, we introduce the datasets and models used in our evaluation. Due to the space limitation, we put the details of hyperparameters and environment in Appendix A.

### A. Datasets

Real-world VFL datasets [60]–[62] are proprietary and cannot be publicly accessed. Therefore, we choose to evaluate on public datasets instead. Specifically, we pick up six datasets, including three image datasets, two tabular datasets, and one text dataset: 1) MNIST [63] is the most popular benchmark for evaluation, which has a training set of 60,000 examples and a test set of 10,000 examples; 2) CIFAR10 [64] is another public dataset for image classification, which consists of 60,000 images with 10 classes; 3) FER [65] is used for facial expression recognition, which consists of a training set of 28,709 examples and a test set of 7178 examples; 4) Company Bankruptcy Prediction Dataset (denoted by CBPD) [66] was collected from the Taiwan Economic Journal for the years from 1999 to 2009, which consists of 6,819 instances with 95 attributes and 2 classes; 5) CRITEO [67] is used for Click-Through-Rate (CTR) prediction, which consists of 100,000 instances; 6) IMDB [68] is widely used in text analysis, consisting of a training set of 25,000 reviews and a test set of 25,000 reviews.

We remove the categorical features in CBPD and CRITEO, as it helps improve the performance from the practices of Kaggle<sup>1</sup> (a community hosting competitions on data science),

<sup>1</sup><https://www.kaggle.com>

and the results of our experiments. Furthermore, since CBPD and CRITEO are quite imbalanced in different classes, we use over-sampling method to balance the number of samples in each category. Then, we split the training and test dataset with a ratio of 7 : 3.

In addition, to simulate VFL scenario, we have to partition the features vertically, following [21], [23], [24]. For images, if two parties hold the same ratio of features, we split them from the center to keep each of parties have the same number of columns. For tabular data, we adopt the same operation and keep the parties have the same number of attributes. We make a little difference for texts because of the lengths of reviews are different in IMDB. Therefore, we set different length of sentences for each party to show their difference in features. If the features are evenly distributed, we let each party hold the same length of sentences.

### B. Models

Since *HashVFL* separates out the bottom model, it is free to choose different models in training. In our evaluation, we use ResNet [55] for processing images, BERT [69] for processing texts, and multilayer perceptron (MLP) [70] for processing tabular data. As for the top model, since its function is to calculate the posteriors of the submitted hash codes, which is not very complex, we also use an MLP with 1 hidden layer.

In addition, we download pretrained ResNet and BERT from PyTorch<sup>2</sup> and Hugging Face<sup>3</sup> respectively and then fine-tune their parameters in the training. Such an operation saves us a lot of computational resources and time.

## V. EVALUATION

In this section, we first evaluate our proposed framework on the performance of specific tasks. Then, we show *HashVFL*'s defensive performance against data reconstruction attack, and the detection performance of abnormal inputs. Finally, we discuss the necessity of integrating differential privacy (DP) [71], [72], which is a widely used privacy preserving technique.

### A. Performance Evaluation

We evaluate *HashVFL* under a strict condition, where we set the length of hash code just enough to cover the number of classes, i.e.,  $len(\mathbf{h}) = \lceil \log_2 C \rceil$ , where  $\lceil \cdot \rceil$  is the ceiling function, and  $C$  is the number of classes. For example, we set the length of the hash code as 4 bits on CIFAR10. Hence, 16 hash codes cover exactly 10 classes. This setting is to minimize the risk of information leakage.

Table II summarizes the performance of *HashVFL* on different datasets. From it, we can find that on three image datasets, *HashVFL* maintains the performance compared to the results without defense. Specifically, on MNIST, the loss of accuracy on the test set is 1.24%, which is the least. On CIFAR10, the loss of accuracy on the test set is 5.39%, which is the largest. The results on IMDB follow the image datasets' conclusion, whose loss of accuracy on the test set is 2.92%.

<sup>2</sup><https://pytorch.org>

<sup>3</sup><https://huggingface.co>

The results on CBPD and CRITEO show that our design can even improve the performance of tabular data. On CRITEO, the accuracy with defense achieves 72.94%, which is higher than 70.72% of the case without defense. We speculate that it is because with such a strict length of codes, i.e., 1, the sign of the value may better reflect the sample’s category, as it pulls the distance between positive and negative classes in disguise.

In summary, our proposed *HashVFL* satisfies the requirement of maintaining the performance of the main task and can apply to different data types.

TABLE II  
EVALUATION RESULTS OF *HashVFL* ON DIFFERENT DATASETS. THE CELL CONTAINS THE ACCURACY (%) ON THE TEST SET.

Dataset	MNIST	CIFAR10	FER	CBPD	CRITEO	IMDb
Without Defense	98.99	76.22	55.93	50.30	70.72	73.64
With Defense	97.75	70.83	51.11	69.34	72.94	69.72

### B. Defensive Performance against Reconstruction Attacks

In this section, we evaluate *HashVFL*’s defensive performance against data reconstruction attacks. Specifically, we assume the strongest adversary, who has all knowledge of the victim party’s bottom model and the target sample’s hash code. Then, we analyze *HashVFL*’s efficacy from two perspectives.

First, we conclude that the adversary cannot reconstruct a specific target sample’s intermediate calculation and corresponding features, even if he/she has full knowledge. The reason is that we only preserve the sign of each bit, which guarantees that no specific values will be leaked.

Second, considering that samples whose hash codes are the same may share a few common features, we also evaluate the situation where the adversary tries to recover some features through hash collision.

We evaluate *HashVFL*’s defense performance on MNIST, CIFAR10, and FER, as the image reconstruction is the most intuitive. Then, we follow the practice in [31] to perform the attack. Since our threat model assumes the adversary knows the bottom model, we then focus on reconstructing features using the following formula:

$$\tilde{\mathbf{x}}^* = \arg \min_{\tilde{\mathbf{x}}} MSE(f_{\theta}(\tilde{\mathbf{x}}), \mathbf{o}_y) + \lambda TV(\tilde{\mathbf{x}}),$$

where  $\tilde{\mathbf{x}}^*$  is the generated sample;  $f_{\theta}(\cdot)$  denotes the bottom model;  $MSE(\cdot)$  calculates two vectors’ mean square error;  $\mathbf{o}_y$  denotes the target class  $y$ ’s corresponding binary code;  $TV(\cdot)$  denotes the Total Variation (TV) term [48];  $\lambda$  is a coefficient to modify the weight of TV term. Specifically, the TV term is calculated as follows:

$$TV(\mathbf{x}) = \sum_{i,j} \sqrt{\|\mathbf{x}_{i+1,j} - \mathbf{x}_{i,j}\|^2 + \|\mathbf{x}_{i,j+1} - \mathbf{x}_{i,j}\|^2},$$

where  $i$  and  $j$  denote the pixel indices. The function of the TV term is to smooth the noise of  $\tilde{\mathbf{x}}^*$ .

For each class’s code, we run 3,000 rounds to reconstruct its data. Furthermore, we vary the hash code length from 4 bits to 16 bits to see if a longer code will leak more information.

Figure 3 plots the reconstructed results on MNIST. Due to the space limitation, we put the results on CIFAR10 and FER in Appendix B.

From the results, we can conclude that even with the strongest assumption, the adversary cannot recover valid information. In addition, the length does not have an evident impact on the reconstruction process.

In summary, *HashVFL* can defend against existing data reconstruction attacks in VFL. The one-way nature of hashing perfectly solves the risk of data being reconstructed.

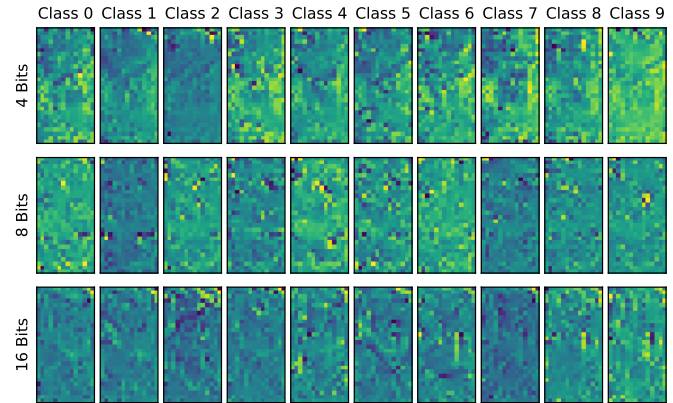


Fig. 3. Reconstruction results on MNIST. The first row shows the reconstructed results with 4 bits hash code on different classes. The second and third rows show 8 and 16 bits, respectively.

### C. Detection Performance of Abnormal Inputs

In this section, we further analyze another advantage of *HashVFL*. We speculate that *HashVFL* can provide an efficient way to detect abnormal inputs since our consistency requires that each party’s code be identical. Specifically, we want to verify that if the hamming distance between two parties’ codes is larger than half of the length, then there may be one party who is cheating.

We evaluate *HashVFL*’s detection ability under the two-party scenario where each party holds half of the features. For each class, we first fix one party’s code, denoted by  $P_{initiator}$ , as the corresponding pre-defined binary code. Then, we vary the other party’s, denoted by  $P_{participate}$ , code to see if there are differences between correct and wrong predictions. Ideally, the correct predictions’ hamming distance between  $P_{initiator}$  and  $P_{participate}$ ’s codes should be less than half of the length, while the wrong predictions’ should be larger than that. It means that if a malicious party wants to change the prediction, he/she must change at least half of the bits to succeed. In addition, we vary the hash code’s length from 4 to 16 bits.

Table III summarizes the results when the hash code is 4 bits. Considering the space limitation, we put the results of 8 bits and 16 bits in Appendix C. From the column of ‘Average’, we can see that *HashVFL* does detect abnormal inputs. If the hamming distance between two parties’ code is larger than half the length, i.e., 2 in this case, the prediction is probably

TABLE III  
DETECTION PERFORMANCE ANALYSIS OF 4 BITS HASH CODE. THE CELL BELONGING TO THE COLUMNS OF ‘CLASS’ REPORTS THE AVERAGED HAMMING DISTANCE BETWEEN TWO HASH CODES. THE COLUMN ‘AVERAGE’ REFERS TO THE AVERAGED RESULTS OF THE CLASSES.

Dataset		Class										Average
		0	1	2	3	4	5	6	7	8	9	
MNIST	correct	0.67	1.57	1.50	1.20	1.00	1.20	1.17	1.75	1.33	1.70	1.31
	error	2.31	2.33	2.50	2.36	2.23	2.36	2.50	2.25	2.40	2.50	2.38
CIFAR10	correct	1.00	<b>2.10</b>	<b>3.00</b>	1.43	1.00	1.67	1.43	1.50	1.20	1.62	1.59
	error	2.33	<b>1.83</b>	<b>1.67</b>	2.44	2.33	2.43	2.44	2.50	2.36	2.38	2.27
FER	correct	2.00	2.00	1.90	0.67	1.29	1.93	1.00				1.35
	error	2.00	2.00	2.17	2.31	2.56	2.50	2.33				2.27
CBPD	correct	1.87	<b>2.00</b>									1.94
	error	<b>4.00</b>	-									4.00
CRITEO	correct	1.87	<b>2.00</b>									1.94
	error	<b>4.00</b>	-									4.00
IMDb	correct	1.87	<b>2.00</b>									1.94
	error	<b>4.00</b>	-									4.00

wrong. For the detailed results of each class, most of them also follow the conclusion. However, on CIFAR10, there are two exceptions in the class ‘1’ and ‘2’ results. We examine the results and find that in these two cases, wrong predictions are concentrated on specific classes, e.g., many wrong predictions on class ‘1’ give class ‘5’, and on class ‘2’ give class ‘8’. Furthermore, the pre-defined codes of class ‘1’ and class ‘5’ are  $[-1, 1, 1, 1]$  and  $[1, 1, 1, 1]$ , whose hamming distance is relatively small. Therefore, the average hamming distance of wrong predictions is smaller in such two cases.

The conclusion is consistent with the results on CBPD, CRITEO, and IMDb. Moreover, we find that the top model is sensitive to the pre-defined binary codes. We speculate that it is because there are only two target codes appear in training for these binary tasks, leaving 14 codes rarely showing. Hence, the top model ‘memorizes’ these two codes. If we let  $P_{initiator}$  submit one of them, the top model will always give the corresponding prediction. Only when two target binary codes appear the top model may be affected. Furthermore, we find that class ‘1’ is more dominant in the prediction than class ‘0’. Therefore, when the code is fixed as class ‘1’’, the prediction is always correct, causing the average distance of correct predictions to be 2. In Table III, we use ‘-’ to denote the situation where the wrong prediction does not occur.

In summary, we find that *HashVFL* helps detect the abnormal inputs by calculating the hamming distance between different parties’ uploaded hash codes. Specifically, if the hamming distance is larger than half of the length, it is most likely that one of them is cheating in the inference.

#### D. Analysis of Integrating Differential Privacy

In this section, we discuss whether it is necessary to additionally use differential privacy (DP) [71], [72] in our current scheme, which is a commonly used privacy-preserving technique in DNNs. Indeed, for some frameworks, such as FATE and TF Encrypted, they have adopted DP to further enhance the protection of data.

In [73], Pham et al. proposed a method to integrate DP with binary code:  $\mathbf{h} = \text{Sign}(\text{Sign}(f(\mathbf{x})) + \text{Lap}(\frac{s}{\epsilon}))$ , where  $\mathbf{h}$  is the hash code;  $\mathbf{x}$  is the feature vector;  $f$  is a DNN model;  $s$  is the sensitivity of  $\text{Sign}(\cdot)$ , actually 2 for binary codes;  $\epsilon$  is the privacy budget [71]; and  $\text{Lap}(\cdot)$  is the Laplace distribution sampling function.

From this design, if  $|\text{Lap}(\frac{2}{\epsilon})| < 1$ , then  $\mathbf{h} = \text{Sign}(f(\mathbf{x}))$ . Furthermore, the probability of  $|\text{Lap}(\frac{2}{\epsilon})| < 1$  can be calculated as:  $\Pr[|\text{Lap}(\frac{2}{\epsilon})| < 1] = 1 - [\text{cdf}(1) - \text{cdf}(-1)] = 1 - e^{-\frac{\epsilon}{2}}$ , where  $\text{cdf}(\cdot)$  denotes the cumulative distribution function of Laplace.

However, the derivation result also reveals a problem that the added noise cannot change the value of one bit when the privacy budget  $\epsilon$  is large. Specifically, following the above calculation, we have  $\Pr[|\text{Lap}(\frac{2}{\epsilon})| \geq 1] = e^{-\frac{\epsilon}{2}}$ . Consider that there is half chance that the sign of the noise is the same as the bit, the probability of flipping one bit’s sign is  $\frac{1}{2}e^{-\frac{\epsilon}{2}}$ . When we set  $\epsilon = 10$ , the probability decreases rapidly to 0.33%, which almost does not provide any privacy protection. In such a situation, the adversary can use the received hash code as the real value, and there is almost no error.

We also explore the effect of integrating DP in *HashVFL* on the main task. Due to the space limitation, we put the details in Appendix D. The conclusion is that the added noise will cause the performance of the main task to degrade. Therefore, we do not recommend integrating DP in *HashVFL* as it reduces accuracy and has a limited defensive effect.

## VI. SENSITIVITY ANALYSIS

In this section, we further evaluate the impact of the default setting in the previous experiments. Specifically, we answer the research questions as follows.

- **Q1:** How does the *number of parties* affect *HashVFL*?
- **Q2:** How does the *length of hash codes* affect *HashVFL*?
- **Q3:** Will different *model architectures* affect *HashVFL*?
- **Q4:** How does different *feature ratios* affect *HashVFL*?
- **Q5:** How does the *number of classes* affect *HashVFL*?

### A. Number of Parties (Q1)

In this section, we evaluate the impact of the number of parties. Since we split the features of the samples on a dataset to simulate a multi-party scenario, the number of features that each party can share will decrease with the number of parties increase. If a party’s features contain almost no valid information, e.g., many columns are black in MNIST, its participation may bring uncertainty to the analysis. Therefore, we decide to conduct experiments on CIFAR10, FER, CBPD, and CRITEO. We do not test on IMDb because BERT takes too much memory to run the experiments; thus, our devices cannot afford the cost of many BERTs running simultaneously.

We let each party hold the same ratio of features, which only differs when rounding. For example, when the number of parties is 3, the feature ratios are 30%, 30%, and 40%. Moreover, considering that the small ratio of features may cause a loss in accuracy, we set the length of hash codes as 16 bits to reduce the impact. Figure 4 plots the results.



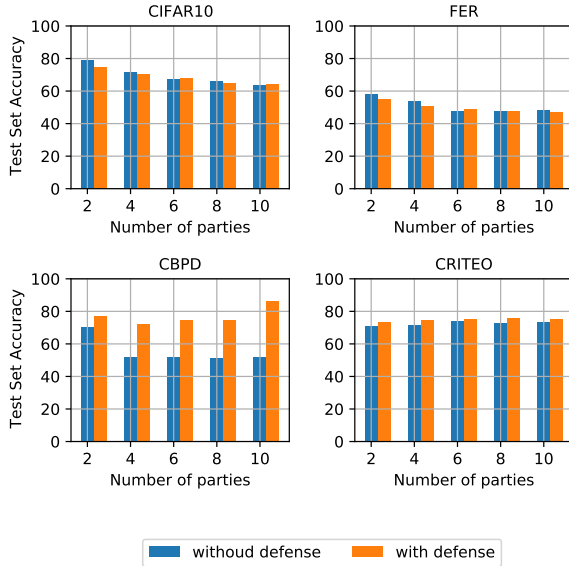


Fig. 4. Analysis of the number of parties. The x-axis represents the number of parties. The y-axis represents the accuracy of the test set.

On CIFAR10 and FER, we can see that the performance decreases with the number of parties increases. It is expected since if we split a useful feature, e.g., an eye or a nose, into many parts, the integrity of the information is then destroyed. In contrast, for CBPD and CRITEO, the performance does not change obviously. It is because the features of tabular data are more independent of each other than image data.

However, if we consider the loss of accuracy when using *HashVFL*, the results in Figure 4 show that our proposed framework maintains the performance well. Our method can even improve the performance for tabular datasets, which is consistent with our findings in Section V-A.

In summary, though the number of parties will affect the performance of the main task, our *HashVFL* can keep close to the performance without defense.

### B. Length of Hash Codes ( $Q_2$ )

This section evaluates the impact of the length of hash codes. Specifically, we double the length of hash codes from 4 to 128 for all datasets. Then, we evaluate the two-party case, each of which holds half features.

Table IV summarizes the performances with different lengths. From the results in Table IV, an apparent conclusion is that with the increase of the length, the performance improves at first and then converges. We speculate that the improvement in the previous stage is because the increased bits can compensate for the information loss caused by hashing, and when the information that the model can extract is saturated, more bits can only cause redundancy.

In summary, we recommend that in *HashVFL*, the length should be determined according to the specific security level in practice. Specifically, longer hash codes mean better performance, while shorter hash codes mean stricter data protection.

TABLE IV  
PERFORMANCE COMPARISON WITH DIFFERENT LENGTHS. THE CELL REPORTS THE ACCURACY (%) ON THE TEST SET.

Dataset	4 Bits	8 Bits	16 Bits	32 Bits	64 Bits	128 Bits
MNIST	97.75	98.34	98.42	98.59	98.42	98.57
CIFAR10	70.83	73.65	74.96	76.14	75.34	75.03
FER	52.73	54.50	55.00	55.66	55.34	55.61
CBPD	70.98	76.62	77.35	77.95	81.64	85.00
CRITEO	73.70	73.13	73.32	74.08	74.48	74.67
IMDb	68.59	72.10	72.66	73.10	73.46	73.59

TABLE V  
PERFORMANCE COMPARISON OF USING MODELS THAT DIFFER IN DEPTH AS THE BOTTOM MODEL. THE CELL REPORTS THE ACCURACY (%).

Dataset		ResNet18	ResNet34	ResNet50
CIFAR10	without defense	76.22	76.96	76.03
	with defense	70.83	71.86	71.20
FER	without defense	56.66	55.59	54.56
	with defense	52.73	52.13	49.62

### C. Architecture of Models ( $Q_3$ )

In this section, we evaluate the impact of the architecture of models. Previous experiments on the different types of models have proved *HashVFL*'s scalability of supporting different models. We want to further answer a research question on how models' capability affects *HashVFL*. Therefore, we use a family of models to experiment. For example, we choose ResNet18, ResNet34, and ResNet50 as the different bottom models in comparison and use MLPs with different hidden layers as the different top models. In general, a deeper model is better for extracting valid information. We evaluate the factor under a two-party scenario; each party holds half of the features. The length of hash codes is fixed as 4 bits. Furthermore, the corresponding datasets used in the evaluation are CIFAR10 and FER. We do not use MNIST since ResNet18 performs well enough on it.

**Bottom Model with Different Architectures.** Table V summarizes the results of the bottom models with different depths. From the results, we find that ResNets with different layers do not affect the performances of cases without defense and with defense. We speculate that it may be because, on the one hand, our limitation of 4 bits may constrain the power of the deeper models; on the other hand, the complexity of the task may also cause a bottleneck.

Furthermore, the loss of accuracy is also stable when we use different bottom models. Combining the results in Table IV, we conclude that in *HashVFL*, the length of the hash codes plays a more critical role than the depth of the bottom model, especially after bottlenecks appear for a given length.

**Top Model with Different Architectures.** Table VI summarizes the results of the top model with different numbers of hidden layers. The results show that the number of hidden

TABLE VI

PERFORMANCE COMPARISON OF USING MODELS THAT DIFFER IN DEPTH AS THE TOP MODEL. THE CELL REPORTS THE ACCURACY (%).

Dataset		1 Layer	2 Layers	3 Layers
CIFAR10	without defense	76.22	76.68	75.47
	with defense	70.83	70.18	71.06
FER	without defense	56.66	55.59	54.56
	with defense	52.73	51.92	51.48

layers does not obviously impact the performance. Also, the loss of performance is not affected. We speculate that the MLP with one hidden layer is enough to approximate the final prediction function of the uploaded embedding in the two-party scenario. Therefore, the increase in depth will not improve the performance.

#### D. Feature Ratio (Q4)

In this section, we evaluate the impact of the feature ratio. Feature ratio refers to the ratio of the number of features owned by a party to all features. Specifically, we conduct the experiments in the two-party scenario and vary one party’s feature ratio from 10% to 50%. In the two-party case, we speculate that varying feature ratios from 60% to 90% is symmetric to the above setting. Therefore, we do not repeat the corresponding experiments.

Figure 5 shows the results. We find that on CIFAR10 and FER, the performances without defense and with defense decrease when the feature ratio increases. It is expected as when the feature ratio increases, another party’s completeness of the image begins to reduce. Furthermore, most of the important features in an image are concentrated in the middle region. Therefore, the partition of important features may cause difficulty in inference, which is consistent with our analysis in Section VI-A.

However, features in CBPD and CRITEO are much more independent, e.g., an attribute will not be split into two parts. Therefore, the change in performance is not obvious with the increase of feature ratio. However, there are some fluctuations.

As for the loss of accuracy, the results on CIFAR10 and CRITEO show that *HashVFL* maintains the performance within an acceptable range, while on CBPD and CRITEO, *HashVFL* can even improve the performance. As we analyzed previously in Section V-A, we speculate that the improvement may be that the binarized code can save the top model from learning from the original embeddings’ floating numbers.

In summary, evaluation results of the feature ratio reveals that in *HashVFL*, complete and valid features are important to reduce the accuracy loss.

#### E. Number of Classes (Q5)

In this section, we further evaluate the impact of the number of classes. Specifically, we choose to conduct experiments on CIFAR10 and CIFAR100 for comparison since they share

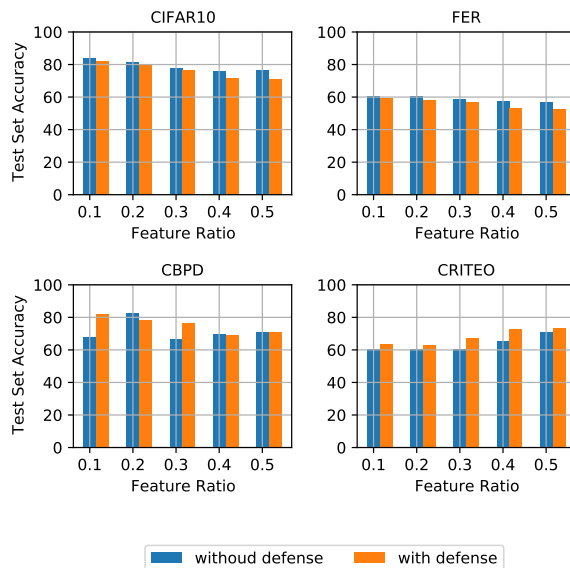


Fig. 5. Analysis of the feature ratios. The x-axis represents the ratio of features held by one party. The y-axis denotes the accuracy (%).

TABLE VII

PERFORMANCE COMPARISON WITH DIFFERENT NUMBERS OF CLASSES. WE PLOT THE RESULTS OF CIFAR10 WITH DEFENSE FOR REFERENCE.

Dataset		8 Bits	16 Bits	32 Bits	64 Bits	128 Bits
CIFAR100	without defense	33.99	34.09	34.75	33.39	34.41
	with defense	24.23	29.51	33.31	33.77	31.96
CIFAR10	with defense	73.65	74.96	76.14	75.34	75.03

the same data but a different number of classes. Table VII summarizes the results.

From the results, an apparent conclusion is that the number of classes does make the task much harder, and our models can only achieve the highest accuracy of 33.77% on the test set when the length is 64 bits with defense, while with the same length, the accuracy is 75.34% on CIFAR10.

Furthermore, when the length is small, we can find that the accuracy loss is much larger than that on CIFAR10. For example, when the length is 8 Bits, the accuracy loss on CIFAR100 is about 10%, while on CIFAR10, the loss is about 6% in Table II. However, if we expand the length of the codes, e.g., 32 bits and 64 bits, the loss of accuracy is acceptable, which is less than 1%.

Therefore, we conclude that a large number of classes will increase the complexity of the main task and thus cause a considerable loss of accuracy when the length of the hash codes is small. However, *HashVFL* can maintain the performance with an acceptable loss of accuracy when there are sufficient bits.

## VII. ABLATION STUDY

We propose three challenges in Section I. Previous works [33], [51], [53] on deep hashing provided a feasible solution on addressing learnability. Therefore, in this section, we explore

the role of two other challenges in *HashVFL*. Specifically, we answer the two research questions as follows.

- **S1:** What is the role of *bit balance* in *HashVFL*?
- **S2:** What else does the *consistency* bring in *HashVFL*?

#### A. Bit Balance (S1)

In Section III, we mention that the BN layer is mandatory in *HashVFL*. In this section, we demonstrate its necessity experimentally. We evaluate the two-party scenario, where each party holds half of the features.

We choose Greedy Hash, proposed by Su et al. [33], as the baseline. Greedy Hash also used the *Sign* function for binarization and combined the STE for gradient estimation. However, Greedy Hash was proposed to address the challenge in retrieval tasks. Su et al. focused on expanding the hash code’s length to improve the retrieval performance and reduce the impact of hash collision. Therefore, they did not need to consider the leverage of each bit, let alone combining the batch normalization in Greedy Hash.

Moreover, there is one more difference between our design and Greedy Hash. Greedy Hash’s loss function adds a penalty function of the Euclidean distance between the embeddings and their corresponding binary codes. The operation forces the embeddings to get close to the binary codes and thus makes them discriminative. However, *HashVFL* has pre-defined the target binary codes to address consistency. Therefore, we use the cosine distance between the hash codes and their corresponding target binary codes instead, which saves us from calculating the Euclidean distance.

Table VIII summarizes the results. On MNIST, CIFAR10, and FER, the performances of Greedy Hash and ours without a BN layer are close. However, after combining a BN layer, it can be seen that the performance improves obviously. For example, on CIFAR10, when the code is 16 bits, our method with a BN layer achieves the highest accuracy of 74.96%. It is expected since the batch normalization can use each bit in the limited length better.

Our method with a BN layer also performs best on CBPD, CRITEO, and IMDB. However, there is a little difference in the comparison between Greedy Hash and our method without batch normalization. On these three datasets, our method without batch normalization almost fails. The different loss function designs cause the difference. Specifically, in Greedy Hash, the loss of Euclidean distance will not directly change the direction of the embeddings but extend or compress its Euclidean norm. Only the gradients calculated by the classification loss will change their directions. However, our optimization of the cosine similarity will rotate the embeddings in the hash space. Furthermore, the rotation angle is also fixed since the target codes are fixed in the hash space. For example, when the hash code length is 4 bits in the binary classification task, there are  $2^4 \cdot 2 = 32$  rotation angles in the optimization. Compared to the change of the gradients from the classification loss, the rotation caused by the similarity loss may be too large, which causes one sample’s hash code to flip at every optimization step. Therefore, it is hard for the

TABLE VIII  
ABLATION STUDY OF BATCH NORMALIZATION’S IMPACT. ‘GREEDY HASH’ DENOTES THE BASELINE FOR REFERENCE. ‘OURS’ REFERS TO OUR DESIGN. THE CELL REPORTS THE ACCURACY (%) ON THE TEST SET.

Dataset	Method		4 Bits	8 Bits	16 Bits
MNIST	Greedy Hash		96.24	97.17	97.82
	Ours	without BN	96.75	97.24	97.02
		with BN	97.75	98.34	98.42
CIFAR10	Greedy Hash		55.53	63.57	61.52
	Ours	without BN	60.44	63.24	60.26
		with BN	70.83	73.65	74.96
FER	Greedy Hash		40.42	42.24	44.65
	Ours	without BN	37.95	45.74	48.68
		with BN	52.73	54.50	55.00
CBPD	Greedy Hash		61.57	63.13	62.42
	Ours	without BN	48.74	49.89	48.56
		with BN	70.98	76.62	77.35
CRITEO	Greedy Hash		63.21	66.94	68.63
	Ours	without BN	49.76	49.93	49.94
		with BN	73.70	73.13	73.32
IMDb	Greedy Hash		70.71	70.63	70.55
	Ours	without BN	50.59	50.34	50.26
		with BN	68.59	72.10	72.66

top model to learn a stable function to give the prediction. However, adding the BN layer can reduce the impact as it evenly divides the distribution of each bit for every batch, which means there is a larger range for each bit to vary without flipping its sign.

In summary, bit balance is an important factor that should be considered, and a BN layer is mandatory in *HashVFL*.

#### B. Consistency (S2)

In Section I, we introduce the challenge of consistency in VFL. The benefit of saving the computation resource and speeding up the training is obvious since we reduce the complexity of calculating the distance between two parties from  $O(N^2)$  to  $O(N)$ . Moreover, our added consistency loss also avoids calculating Euclidean distance, which is required in [33]. The results in Table VIII show that the performance of such a replacement keeps close to the ones with Euclidean distance constraint.

In this section, we are interested in answering the research question of what else consistency can bring in *HashVFL*. Specifically, we speculate that keeping the consistency helps make the task easier than not, as this constraint can reduce the number of combinations of multi-party’s hash codes.

To verify the speculation, we conduct the experiments as follows. First, like in previous experiments, we choose the two-party scenario for evaluation, each of which has half of the features. Then, since our implementation uses consistency to replace the Euclidean distance loss, we, in turn, integrate the Euclidean distance penalty to ensure normal training. Hence,

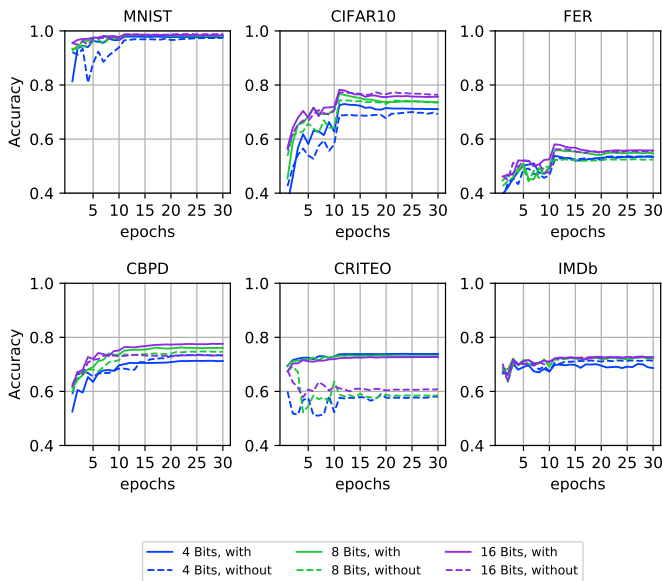


Fig. 6. Performance comparison of addressing the consistency. The x-axis denotes the epoch in training. The y-axis denotes the accuracy (%). ‘with’ and ‘without’ denote the cases of using cosine similarity and not.

we can compare the difference of whether adding the cosine similarity in the loss function.

Figure 6 plots the results. Except for two curves of CBPD and IMDb with 4 bits code, the curves with consistency requirements are higher than those that do not satisfy the requirement with different lengths on all datasets. Specifically, on CRITEO, the advantage of adding the cosine similarity is obvious, where the gap is nearly 15%. However, on other datasets, the performance is higher than that without consideration of consistency, around 1%.

Furthermore, the cosine similarity loss can also accelerate the training. A common phenomenon on all datasets is that in the first 10 epochs, the accuracy will be improved faster by adding the cosine similarity loss than not.

We investigate further and find that after 10 epochs, the accuracy on the training set is still increasing, while the accuracy on the test set decreases. We speculate that there may be overfitting in the next 20 epochs, causing these two ways’ performances to be close. For the training with cosine similarity loss, the accuracy on the test set decreases after 30 epochs. In contrast, for the training without cosine similarity loss, the accuracy of the test set is improved.

In summary, addressing consistency also helps improve and accelerate the training in *HashVFL*. Combining the benefits of detecting the abnormal inputs and saving the cost of calculating Euclidean distance, we conclude that this factor is also essential in *HashVFL*.

## VIII. RELATED WORK

In this section, we supplement the related work, as well as a comparison of the work we refer to and our method.

### A. Learning to Hash

Nearest neighbor search is a time-honored problem that aims to find the samples in the database with the smallest distance from them to the queries. Hashing is a popular solution for its computational and storage efficiency. With the development of DNNs, learning to hash, also called deep hashing, shows more advantages than conventional methods. There are many ways to classify existing deep hashing methods [74], [75]. In this section, we mainly discuss deep supervised hashing [33], [38], [39], [51]–[53], [76]–[78].

A line of work in the domain of deep supervised hashing aims to solve the binary optimization, specifically how to address the vanishment of gradients. In [53], Cao et al. proposed a hashing mechanism based on *tanh* and *sigmoid*, as these two functions are differentiable. Then, the hash code can be generated at reference time by clipping the activations with a threshold. Li et al. [77] did not directly apply binarizing function in DNNs, but designed a specific penalty function to generate features as binary as possible. In [33], Su et al. proposed the *Sign* function to directly binarize the features. Then, they used *straight-through estimator* to estimate the vanishing gradients.

Another line of work tries to learn hashing from a new perspective. In [38], Fan et al. used a random assignment scheme to generate target vectors with maximal inter-class distance. Then, they optimized the distance between the embeddings and the vectors. In [79], Yuan et al. used the Hadamard matrix as target centers, then optimized with binary cross-entropy loss. In [39], Hoe et al. revealed the connection between cosine similarity and Hamming distance and integrated the category information into one loss. In addition, these works do not binarize the embeddings in training.

### B. Attacks in Vertical Federated Learning

Recently, several works studied the security of VFL. There are mainly two streams of them: data privacy and security.

For privacy, Luo et al. [21] proposed a method that used DNNs to reconstruct the data in VFL. Similarly, in [22], Weng et al. also investigated the leakage risks of VFL with more machine learning methods, such as logistic regression [80] and XGBoost [81]. In [23], Qiu et al. revealed the leakage risks of graph data in VFL, which further expanded the range of models. Moreover, Fu et al. [24] investigated the leakage of labels in VFL.

For security, Liu et al. [82] found that the party that owns the label can easily implement the backdoor attack. They further proposed a backdoor attack in VFL by replacing the gradients in training in cases where the adversary has no labels.

### C. Defenses in Vertical Federated Learning

Since VFL is a new paradigm, a few works study the defense in VFL compared to attacks. Specifically, we also introduce two lines of work according to the attacks.

In [29], Sun et al. proposed a scheme to reduce the leakage from data reconstruction attacks, which combined the correlation distance between extracted embeddings and the raw input

into the penalty function. Vepakomma et al. also applied a similar idea in [30]. Sun et al. [83] also proposed a method that integrates DP in the forward process to defend against label inference attacks. In [24], Fu et al. discussed several defenses against label inference attacks by using gradient compression [84]. In addition, in [73], Pham et al. integrated binary neural networks (BNNs) [34] at the first few layers to defend feature reconstruction attack on the feature masks.

In [85], Liu et al. used feature reconstruction to defend the backdoor attack, which applied an attack for good.

#### D. Remark

Our proposed *HashVFL* aims to address the feature reconstruction attack through hashing. Different from the above defenses [29], [30], hashing can directly cut off the correlation between the binarized embedding and the corresponding input. Compared to the BNN-based defense [73], *HashVFL* can handle more complex scenarios, e.g., different types of data, and is easy to assemble into the existing frameworks. Indeed, Pham et al. mainly tried using BNNs to address IoT devices' computation overhead. Furthermore, their defense is not strong since they only applied to binarize at the first few layers on the feature maps.

Research on learning to hash gives us many insights into integrating hashing mechanisms. GreedyHash, proposed by Su et al. [33], provides scalability that best fits VFL for selecting models and data. However, more is needed to solve the challenges of bit balance and consistency. The methods in [53], [77] are also effective in learning to hash. However, they have to transmit embeddings in training, which still leaves the risk of leakage. Therefore, we do not adopt them in *HashVFL*'s design. For the same reason, we do not merely use pre-defined centers [38], [39], [79] to learn the hashing function but combine them for improvement.

## IX. DISCUSSION

### A. Risk of Label Leakage

*HashVFL* achieves good performance in defending against data reconstruction attacks while keeping the loss of accuracy of the main task within an acceptable range. Furthermore, we limit the length of the hash codes to just enough to cover the number of classes.

However, there still leaves the risk of label leakage. With a good bottom model, an honest-but-curious party can easily infer the sample's label with its hash codes. The better the bottom model, the more accurate the inference.

Our evaluation of integrating DP with our hashing mechanism may provide a solution for solving the dilemma, i.e., using a long hash code and adding a strong noise. However, the cost is the loss of accuracy. We leave the exploration of defending against label inference attacks based on *HashVFL* as one of our future works.

### B. Bias Between Parties

In Section VI-D, with a given feature ratio of images, our results show that when one party holds most features,

the performance is better than when two parties both hold half of the features. Our analysis points out that the feature's completeness remains in the former situation, and thus the top model can capture valid information. However, the phenomenon also raises a dilemma that in VFL, the party who holds more features has more importance on the final predictions. *HashVFL* may further strengthen the 'bias' as we erase much information for all parties by using hashing.

A possible risk brought by the bias is that if the dominant party is malicious at inference time, he/she can easily manipulate the final prediction by using the bias. Therefore, how to reduce the bias and make each feature important in the final prediction is a vital research question in applying *HashVFL*. We think this is an open question and a lot of interesting work could be generated in the future.

### C. Data Valuation

In [86], Guan et al. proposed an interpretation method for VFL using Shapley value [87]. The purpose is to measure the feature importance for a prediction in VFL. Hence the host of VFL can value the other parties' contribution to providing features. However, calculating the Shapley value is computationally expensive, especially when there are many features and floating point calculations.

*HashVFL* provides an efficient way to implement Guan's method, as the hash codes are binary, which is easy to calculate. Moreover, for other methods [88], [89] used in data valuation, our design can also speed them up.

### D. Canceling Encryption

As we mentioned earlier in the paper, existing frameworks [40]–[43] use HE to provide the data privacy guarantee, which is proven not sufficient. Indeed, the encryption operation is used to ensure that other parties cannot access the details of the intermediate calculations.

However, this limitation may be relaxed in *HashVFL* since the binarization erases most of the information, especially when we constrain the hash code length to be  $\lceil \log_2 C \rceil$ , where  $C$  is the number of classes. The raw data will not be reconstructed even if an adversary has a sample's hash code and the corresponding bottom model.

Therefore, we speculate that for frameworks using hashing, the encryption operation can be canceled. In addition, by doing so, the efficiency of VFL can be improved a lot, which helps VFL's wider application.

## X. CONCLUSION

This work proposes a hashing-based VFL framework, *HashVFL*. To our best knowledge, this is the first attempt to adopt the hashing mechanism in VFL for defending against data reconstruction attacks. We present three challenges of integrating hashing and provide corresponding solutions. *HashVFL* is evaluated in many different settings and is proven to maintain the main task's performance. In addition to defending against data reconstruction attacks, we experimentally demonstrate *HashVFL*'s efficacy in detecting abnormal

inputs. We hope this work can attract more researchers to find broader application domains of *HashVFL* in the real world.

## REFERENCES

- [1] L. Breiman, *Machine Learning*, vol. 45, no. 1, pp. 5–32, 2001.
- [2] C.-C. Chang and C.-J. Lin, “LIBSVM,” *ACM Transactions on Intelligent Systems and Technology*, vol. 2, no. 3, pp. 1–27, apr 2011.
- [3] Y. LeCun, Y. Bengio, and G. Hinton, “Deep learning,” *Nature*, vol. 521, no. 7553, pp. 436–444, may 2015.
- [4] J. Jumper, R. Evans, A. Pritzel, T. Green, M. Figurnov, O. Ronneberger, K. Tunyasuvunakool, R. Bates, A. Židek, A. Potapenko, A. Bridgland, C. Meyer, S. A. A. Kohl, A. J. Ballard, A. Cowie, B. Romera-Paredes, S. Nikolov, R. Jain, J. Adler, T. Back, S. Petersen, D. Reiman, E. Clancy, M. Zielinski, M. Steinegger, M. Pacholska, T. Berghammer, S. Bodenstein, D. Silver, O. Vinyals, A. W. Senior, K. Kavukcuoglu, P. Kohli, and D. Hassabis, “Highly accurate protein structure prediction with AlphaFold,” *Nature*, vol. 596, no. 7873, pp. 583–589, jul 2021.
- [5] L.-C. Chen, G. Papandreou, I. Kokkinos, K. Murphy, and A. L. Yuille, “DeepLab: Semantic image segmentation with deep convolutional nets, atrous convolution, and fully connected CRFs,” *IEEE Transactions on Pattern Analysis and Machine Intelligence*, vol. 40, no. 4, pp. 834–848, apr 2018.
- [6] C. Shorten and T. M. Khoshgoftaar, “A survey on image data augmentation for deep learning,” *Journal of Big Data*, vol. 6, no. 1, jul 2019.
- [7] Z. Wu, S. Pan, F. Chen, G. Long, C. Zhang, and P. S. Yu, “A comprehensive survey on graph neural networks,” *IEEE Transactions on Neural Networks and Learning Systems*, vol. 32, no. 1, pp. 4–24, jan 2021.
- [8] A. J. Dautel, W. K. Härdle, S. Lessmann, and H.-V. Seow, “Forex exchange rate forecasting using deep recurrent neural networks,” *Digital Finance*, vol. 2, no. 1-2, pp. 69–96, mar 2020.
- [9] M. Dixon, D. Klabjan, and J. H. Bang, “Classification-based financial markets prediction using deep neural networks,” *Algorithmic Finance*, vol. 6, no. 3-4, pp. 67–77, dec 2017.
- [10] Q. Wang, Y. Zhou, T. Ruan, D. Gao, Y. Xia, and P. He, “Incorporating dictionaries into deep neural networks for the chinese clinical named entity recognition,” *Journal of Biomedical Informatics*, vol. 92, p. 103133, apr 2019.
- [11] S. Krebs, B. Duraisamy, and F. Flohr, “A survey on leveraging deep neural networks for object tracking,” in *2017 IEEE 20th International Conference on Intelligent Transportation Systems (ITSC)*. IEEE, oct 2017.
- [12] I. F. Kupryashkin, “Impact of the radar image resolution of military objects on the accuracy of their classification by a deep convolutional neural network,” *Journal of the Russian Universities. Radioelectronics*, vol. 25, no. 1, pp. 36–46, feb 2022.
- [13] P. Voigt and A. Von dem Bussche, “The eu general data protection regulation (gdpr);” *A Practical Guide, 1st Ed., Cham: Springer International Publishing*, 2017.
- [14] D. Kiselbach and C. E. Joern, “New consumer product safety laws in canada and the united states: Business on the border,” *Global Trade and Customs Journal*, vol. 7, no. 1, 2012.
- [15] J. Xu, B. S. Glicksberg, C. Su, P. Walker, J. Bian, and F. Wang, “Federated learning for healthcare informatics,” 2020.
- [16] A. Hard, K. Rao, R. Mathews, S. Ramaswamy, F. Beaufays, S. Augenstein, H. Eichner, C. Kiddon, and D. Ramage, “Federated learning for mobile keyboard prediction,” 2018.
- [17] Q. Yang, Y. Liu, T. Chen, and Y. Tong, “Federated machine learning: Concept and applications,” *ACM Transactions on Intelligent Systems and Technology (TIST)*, vol. 10, no. 2, pp. 1–19, 2019.
- [18] T. S. Brisimi, R. Chen, T. Mela, A. Olshevsky, I. C. Paschalidis, and W. Shi, “Federated learning of predictive models from federated electronic health records,” *International journal of medical informatics*, vol. 112, pp. 59–67, 2018.
- [19] S. Hardy, W. Henecka, H. Ivey-Law, R. Nock, G. Patrini, G. Smith, and B. Thorne, “Private federated learning on vertically partitioned data via entity resolution and additively homomorphic encryption,” *arXiv preprint arXiv:1711.10677*, 2017.
- [20] C. Zhang, S. Li, J. Xia, W. Wang, F. Yan, and Y. Liu, “Batchcrypt: Efficient homomorphic encryption for cross-silo federated learning,” in *2020 USENIX Annual Technical Conference*, 2020, pp. 493–506.
- [21] X. Luo, Y. Wu, X. Xiao, and B. C. Ooi, “Feature inference attack on model predictions in vertical federated learning,” *CoRR*, vol. abs/2010.10152, 2020.
- [22] H. Weng, J. Zhang, F. Xue, T. Wei, S. Ji, and Z. Zong, “Privacy leakage of real-world vertical federated learning,” 2021.
- [23] P. Qiu, X. Zhang, S. Ji, T. Du, Y. Pu, J. Zhou, and T. Wang, “Your labels are selling you out: Relation leaks in vertical federated learning,” *IEEE Transactions on Dependable and Secure Computing*, pp. 1–16, 2022.
- [24] C. Fu, X. Zhang, S. Ji, J. Chen, J. Wu, S. Guo, J. Zhou, A. X. Liu, and T. Wang, “Label inference attacks against vertical federated learning,” USENIX Association, 2022.
- [25] A. Creswell, T. White, V. Dumoulin, K. Arulkumaran, B. Sengupta, and A. A. Bharath, “Generative adversarial networks: An overview,” *IEEE Signal Processing Magazine*, vol. 35, no. 1, pp. 53–65, jan 2018.
- [26] T. Karras, S. Laine, M. Aittala, J. Hellsten, J. Lehtinen, and T. Aila, “Analyzing and improving the image quality of StyleGAN,” in *2020 IEEE/CVF Conference on Computer Vision and Pattern Recognition (CVPR)*. IEEE, jun 2020.
- [27] C. Saharia, W. Chan, H. Chang, C. Lee, J. Ho, T. Salimans, D. Fleet, and M. Norouzi, “Palette: Image-to-image diffusion models,” in *ACM SIGGRAPH 2022 Conference Proceedings*, 2022, pp. 1–10.
- [28] E. Hoogeboom, V. G. Satorras, C. Vignac, and M. Welling, “Equivariant diffusion for molecule generation in 3d,” in *International Conference on Machine Learning*. PMLR, 2022, pp. 8867–8887.
- [29] J. Sun, Y. Yao, W. Gao, J. Xie, and C. Wang, “Defending against reconstruction attack in vertical federated learning,” *CoRR*, vol. abs/2107.09898, 2021.
- [30] P. Vepakomma, A. Singh, O. Gupta, and R. Raskar, “Nopeek: Information leakage reduction to share activations in distributed deep learning,” *CoRR*, vol. abs/2008.09161, 2020.
- [31] Z. He, T. Zhang, and R. B. Lee, “Model inversion attacks against collaborative inference,” *Proceedings of the 35th Annual Computer Security Applications Conference*, 2019.
- [32] L. Zhao, Q. Wang, C. Wang, Q. Li, C. Shen, and B. Feng, “Veriml: Enabling integrity assurances and fair payments for machine learning as a service,” *IEEE Transactions on Parallel and Distributed Systems*, vol. 32, pp. 2524–2540, 2021.
- [33] S. Su, C. Zhang, K. Han, and Y. Tian, “Greedy hash: Towards fast optimization for accurate hash coding in cnn,” in *Advances in Neural Information Processing Systems*, S. Bengio, H. Wallach, H. Larochelle, K. Grauman, N. Cesa-Bianchi, and R. Garnett, Eds., vol. 31. Curran Associates, Inc., 2018.
- [34] H. Qin, R. Gong, X. Liu, X. Bai, J. Song, and N. Sebe, “Binary neural networks: A survey,” *ArXiv*, vol. abs/2004.03333, 2020.
- [35] Y. Bengio, N. Léonard, and A. C. Courville, “Estimating or propagating gradients through stochastic neurons for conditional computation,” *ArXiv*, vol. abs/1308.3432, 2013.
- [36] P. Yin, J. Lyu, S. Zhang, S. J. Osher, Y. Qi, and J. Xin, “Understanding straight-through estimator in training activation quantized neural nets,” in *International Conference on Learning Representations*, 2019.
- [37] S. Ioffe and C. Szegedy, “Batch normalization: Accelerating deep network training by reducing internal covariate shift,” in *Proceedings of the 32nd International Conference on International Conference on Machine Learning - Volume 37*, ser. ICML’15. JMLR.org, 2015, p. 448–456.
- [38] L. Fan, K. W. Ng, C. Ju, T. Zhang, and C. S. Chan, “Deep polarized network for supervised learning of accurate binary hashing codes,” in *Proceedings of the Twenty-Ninth International Joint Conference on Artificial Intelligence, IJCAI-20*, C. Bessiere, Ed. International Joint Conferences on Artificial Intelligence Organization, 7 2020, pp. 825–831, main track.
- [39] J. T. Hoe, K. W. Ng, T. Zhang, C. S. Chan, Y.-Z. Song, and T. Xiang, “One loss for all: Deep hashing with a single cosine similarity based learning objective,” in *Advances in Neural Information Processing Systems*, M. Ranzato, A. Beygelzimer, Y. Dauphin, P. Liang, and J. W. Vaughan, Eds., vol. 34. Curran Associates, Inc., 2021, pp. 24286–24298.
- [40] “FATE,” <https://fedai.org>.
- [41] “PySyft,” <https://www.openmined.org>.
- [42] “TF Encrypted,” <https://tf-encrypted.io>.
- [43] B. Knott, S. Venkataraman, A. Hannun, S. Sengupta, M. Ibrahim, and L. van der Maaten, “Crypten: Secure multi-party computation meets machine learning,” in *arXiv 2109.00984*, 2021.

- [44] C. Gentry, “Fully homomorphic encryption using ideal lattices,” in *Proceedings of the forty-first annual ACM symposium on Theory of computing*, 2009, pp. 169–178.
- [45] L. Zhu, Z. Liu, and S. Han, “Deep leakage from gradients,” in *NeurIPS*, 2019.
- [46] D. Pasquini, G. Ateniese, and M. Bernaschi, “Unleashing the tiger: Inference attacks on split learning,” *Proceedings of the 2021 ACM SIGSAC Conference on Computer and Communications Security*, 2021.
- [47] E. Erdogan, A. Kupcu, and A. E. Cicek, “Unsplit: Data-oblivious model inversion, model stealing, and label inference attacks against split learning,” *Proceedings of the 21st Workshop on Privacy in the Electronic Society*, 2021.
- [48] L. I. Rudin, S. Osher, and E. Fatemi, “Nonlinear total variation based noise removal algorithms,” *Physica D: Nonlinear Phenomena*, vol. 60, pp. 259–268, 1992.
- [49] R. L. Rivest, “The md5 message-digest algorithm,” in *RFC*, 1990.
- [50] M. Datar, N. Immorlica, P. Indyk, and V. S. Mirrokni, “Locality-sensitive hashing scheme based on p-stable distributions,” in *SCG '04*, 2004.
- [51] D. Wu, Q. Dai, J. Liu, B. Li, and W. Wang, “Deep incremental hashing network for efficient image retrieval,” in *2019 IEEE/CVF Conference on Computer Vision and Pattern Recognition (CVPR)*. IEEE, jun 2019.
- [52] J. Wang, T. Zhang, J. Song, N. Sebe, and H. T. Shen, “A survey on learning to hash,” *IEEE Transactions on Pattern Analysis and Machine Intelligence*, vol. 40, no. 4, pp. 769–790, apr 2018.
- [53] Z. Cao, M. Long, J. Wang, and P. S. Yu, “Hashnet: Deep learning to hash by continuation,” *2017 IEEE International Conference on Computer Vision (ICCV)*, pp. 5609–5618, 2017.
- [54] A. J. Paverd and A. C. Martin, “Modelling and automatically analysing privacy properties for honest-but-curious adversaries,” 2014.
- [55] K. He, X. Zhang, S. Ren, and J. Sun, “Deep residual learning for image recognition,” *2016 IEEE Conference on Computer Vision and Pattern Recognition (CVPR)*, pp. 770–778, 2016.
- [56] K. Simonyan and A. Zisserman, “Very deep convolutional networks for large-scale image recognition,” *CoRR*, vol. abs/1409.1556, 2015.
- [57] Y. Weiss, A. Torralba, and R. Fergus, “Spectral hashing,” in *NIPS*, 2008.
- [58] M. Charikar, “Similarity estimation techniques from rounding algorithms,” in *STOC '02*, 2002.
- [59] M. Norouzi, D. J. Fleet, and R. Salakhutdinov, “Hamming distance metric learning,” in *NIPS*, 2012.
- [60] A. Hard, C. M. Kiddon, D. Ramage, F. Beaufays, H. Eichner, K. Rao, R. Mathews, and S. Augenstein, “Federated learning for mobile keyboard prediction,” 2018.
- [61] Webank, “A case of traffic violations insurance-using federated learning,” 2020, <https://www.fedai.org/cases>.
- [62] —, “Utilization of FATE in risk management of credit in small and micro enterprises,” 2020, <https://www.fedai.org/cases>.
- [63] Y. LeCun, L. Bottou, Y. Bengio, and P. Haffner, “Gradient-based learning applied to document recognition,” *Proc. IEEE*, vol. 86, pp. 2278–2324, 1998.
- [64] A. Krizhevsky, G. Hinton *et al.*, “Learning multiple layers of features from tiny images,” 2009.
- [65] E. Barsoum, C. Zhang, C. Canton Ferrer, and Z. Zhang, “Training deep networks for facial expression recognition with crowd-sourced label distribution,” in *ACM International Conference on Multimodal Interaction (ICMI)*, 2016.
- [66] D. Liang, C.-C. Lu, C.-F. Tsai, and G.-A. Shih, “Financial ratios and corporate governance indicators in bankruptcy prediction: A comprehensive study,” *European Journal of Operational Research*, vol. 252, no. 2, pp. 561–572, 2016.
- [67] H. Guo, R. Tang, Y. Ye, Z. Li, and X. He, “Deepfm: A factorization-machine based neural network for ctr prediction,” in *IJCAI*, 2017.
- [68] A. L. Maas, R. E. Daly, P. T. Pham, D. Huang, A. Y. Ng, and C. Potts, “Learning word vectors for sentiment analysis,” in *Proceedings of the 49th Annual Meeting of the Association for Computational Linguistics: Human Language Technologies*. Portland, Oregon, USA: Association for Computational Linguistics, June 2011, pp. 142–150.
- [69] J. Devlin, M.-W. Chang, K. Lee, and K. Toutanova, “Bert: Pre-training of deep bidirectional transformers for language understanding,” in *NAACL*, 2019.
- [70] J. Tang, C. Deng, and G. Huang, “Extreme learning machine for multilayer perceptron,” *IEEE Transactions on Neural Networks and Learning Systems*, vol. 27, pp. 809–821, 2016.
- [71] C. Dwork and A. Roth, “The algorithmic foundations of differential privacy,” *Found. Trends Theor. Comput. Sci.*, vol. 9, pp. 211–407, 2014.
- [72] M. Abadi, A. Chu, I. J. Goodfellow, H. B. McMahan, I. Mironov, K. Talwar, and L. Zhang, “Deep learning with differential privacy,” *Proceedings of the 2016 ACM SIGSAC Conference on Computer and Communications Security*, 2016.
- [73] N. D. Pham, A. Abuadba, Y. Gao, T. D. K. Phan, and N. K. Chilamkurti, “Binarizing split learning for data privacy enhancement and computation reduction,” *ArXiv*, vol. abs/2206.04864, 2022.
- [74] J. Wang, T. Zhang, J. Song, N. Sebe, and H. T. Shen, “A survey on learning to hash,” *IEEE Transactions on Pattern Analysis and Machine Intelligence*, vol. 40, pp. 769–790, 2018.
- [75] X. Luo, C. Chen, H. Zhong, H. Zhang, M. Deng, J. Huang, and X. Hua, “A survey on deep hashing methods,” *ACM Transactions on Knowledge Discovery from Data (TKDD)*, 2022.
- [76] H. Liu, R. Wang, S. Shan, and X. Chen, “Deep supervised hashing for fast image retrieval,” *International Journal of Computer Vision*, pp. 1–18, 2016.
- [77] W.-J. Li, S. Wang, and W.-C. Kang, “Feature learning based deep supervised hashing with pairwise labels,” *ArXiv*, vol. abs/1511.03855, 2016.
- [78] Q.-Y. Jiang and W.-J. Li, “Asymmetric deep supervised hashing,” in *AAAI*, 2018.
- [79] L. Yuan, T. Wang, X. Zhang, F. E. H. Tay, Z. Jie, W. Liu, and J. Feng, “Central similarity quantization for efficient image and video retrieval,” *2020 IEEE/CVF Conference on Computer Vision and Pattern Recognition (CVPR)*, pp. 3080–3089, 2020.
- [80] E. R. Ziegel, “The elements of statistical learning,” *Technometrics*, vol. 45, pp. 267 – 268, 2003.
- [81] T. Chen and C. Guestrin, “Xgboost: A scalable tree boosting system,” *Proceedings of the 22nd ACM SIGKDD International Conference on Knowledge Discovery and Data Mining*, 2016.
- [82] Y. Liu, T. Zou, Y. Kang, W. Liu, Y. He, Z. qian Yi, and Q. Yang, “Batch label inference and replacement attacks in black-boxed vertical federated learning,” 2021.
- [83] J. Sun, X. Yang, Y. Yao, and C. Wang, “Label leakage and protection from forward embedding in vertical federated learning,” *ArXiv*, vol. abs/2203.01451, 2022.
- [84] Y. Lin, S. Han, H. Mao, Y. Wang, and W. J. Dally, “Deep gradient compression: Reducing the communication bandwidth for distributed training,” *ArXiv*, vol. abs/1712.01887, 2018.
- [85] J. Liu, “Rvfr: Robust vertical federated learning via feature subspace recovery,” 2021.
- [86] G. Wang, “Interpret federated learning with shapley values,” 2019.
- [87] S. M. Lundberg and S.-I. Lee, “A unified approach to interpreting model predictions,” in *NIPS*, 2017.
- [88] T. Wang, J. Rausch, C. Zhang, R. Jia, and D. X. Song, “A principled approach to data valuation for federated learning,” in *Federated Learning*, 2020.
- [89] X. Han, L. Wang, and J. Wu, “Data valuation for vertical federated learning: An information-theoretic approach,” *ArXiv*, vol. abs/2112.08364, 2021.
- [90] D. P. Kingma and J. Ba, “Adam: A method for stochastic optimization,” *CoRR*, vol. abs/1412.6980, 2015.

## APPENDIX

### A. Experimental Setup

**Hyperparameters.** We set the training epochs for 30 times and an Adam [90] optimizer with a batch size of 256 for images and tabular data, and 8 for texts. The Adam optimizer has the learning rate of  $1e - 3$ , the weight decay of  $5e - 4$ , and a momentum by default in PyTorch’s implementation. In addition, we shrink the learning rate by 10% every 10 epochs. We store the last epoch’s model, which are then used to measure the main task’s performance on the test set.

**Environment.** We implement the attacks in Python and conduct all experiments on a workstation equipped with AMD Ryzen 9 3950X and an NVIDIA GTX 3090 GPU card. We

use PyTorch to implement the models used in the experiments, and pandas<sup>4</sup> and sklearn<sup>5</sup> for data pre-processing.

### B. Defense Performance against Data Reconstruction Attacks

In this section, we further present the reconstructed results on CIFAR10 and FER. Figure 7 shows the results on CIFAR10, and Figure 8 shows the results on FER.

These two figures show that the reconstruction attack cannot recover valid information from the hash code. Furthermore, a longer length will not improve the attack’s performance. The conclusion is consistent with that in Section V-B.

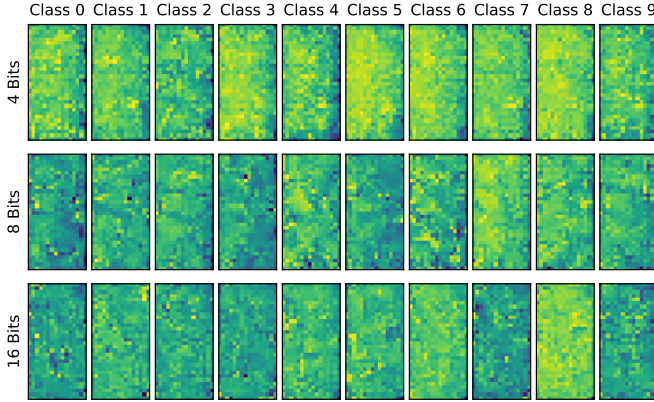


Fig. 7. Reconstruction results on CIFAR10.

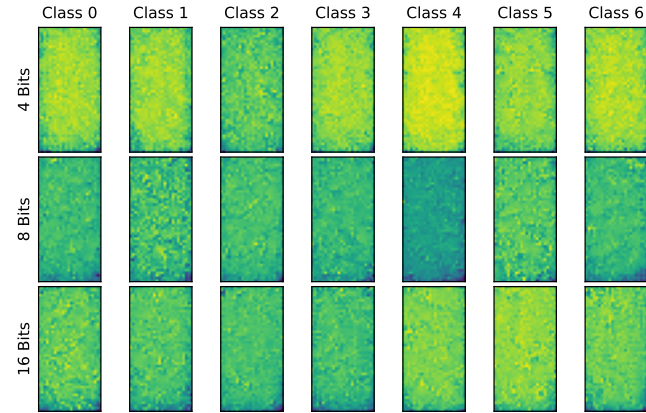


Fig. 8. Reconstruction results on FER.

### C. Detection Performance of Abnormal Inputs

This section presents the detection performance with 8 bits and 16 bits. Table IX summarizes the results of 8 bits. Table X summarizes the results of 16 bits.

From these two tables, we can find that with a longer length, the conclusion is still that the hamming distance of the correct

predictions will not exceed half of the length, while the wrong predictions will. Furthermore, the exception does not appear in these two cases.

TABLE IX  
DETECTION PERFORMANCE ANALYSIS OF 8 BITS HASH CODE. THE CELL REPORTS THE AVERAGE HAMMING DISTANCE BETWEEN TWO HASH CODES.

Dataset		Class										Average
		0	1	2	3	4	5	6	7	8	9	
MNIST	correct	3.43	3.49	3.23	3.78	3.19	3.35	3.73	3.42	3.59	3.42	3.46
	error	5.11	5.29	4.76	4.56	5.09	4.49	4.91	4.89	5.20	4.62	4.89
CIFAR10	correct	3.38	3.65	2.86	3.74	3.32	3.47	3.40	3.00	3.13	3.84	3.38
	error	5.19	5.21	4.48	5.58	5.03	5.11	5.10	4.80	5.00	4.41	4.99
FER	correct	3.52	4.00	3.58	3.11	3.46	3.77	3.69				3.59
	error	5.42	4.00	5.30	4.68	5.22	4.02	5.92				4.94
CBPD	correct	3.85	3.98									3.92
	error	4.14	5.25									4.69
CRITEO	correct	4.00	3.67									3.84
	error	-	5.12									5.12
IMDb	correct	3.93	3.92									3.93
	error	5.60	4.09									4.85

TABLE X  
DETECTION PERFORMANCE ANALYSIS OF 16 BITS HASH CODE. THE CELL REPORTS THE HAMMING DISTANCE BETWEEN TWO HASH CODES.

Dataset		Class										Average
		0	1	2	3	4	5	6	7	8	9	
MNIST	correct	7.77	7.70	7.73	7.79	7.46	7.71	7.46	7.89	7.93	7.29	7.67
	error	10.20	9.89	10.61	9.95	9.53	10.45	9.81	9.82	9.91	9.50	9.97
CIFAR10	correct	7.83	7.33	7.91	7.94	7.80	7.99	7.82	7.76	7.58	7.31	7.72
	error	10.49	9.57	10.02	9.59	10.19	11.57	10.23	10.45	9.98	9.44	10.15
FER	correct	7.90	8.00	7.85	6.80	7.68	7.88	7.67				7.68
	error	9.95	8.00	10.13	9.09	9.27	10.92	10.21				9.65
CBPD	correct	7.80	8.00									7.90
	error	8.14	10.24									9.18
CRITEO	correct	7.96	7.99									7.97
	error	8.92	8.44									8.68
IMDb	correct	7.93	7.85									7.89
	error	10.00	8.63									9.31

### D. Experimental results of Integrating Differential Privacy

To thoroughly analyze the necessity of integrating DP, we further conduct experiments on adding Laplace noise in training. Specifically, we still evaluate the two-party scenario, where each holds half of the features. Table XI summarizes the results.

From the results, we can find that when  $\epsilon = 1$  or  $\epsilon = 2$ , the noise’s impact on the accuracy is apparent. However, when  $\epsilon \geq 10$ , the loss of accuracy is limited. It is expected as the probabilities of flipping one bit’s sign are 30.32% when  $\epsilon = 1$  and 0.33% when  $\epsilon = 10$ . A small probability means that accurate information can be maintained, leading to better performance.

In addition, with the increase in the length of the hash codes, the loss of accuracy decreases. It is natural if we regard the adding noise on each bit as a Bernoulli trial with probability  $\frac{1}{2}e^{-\frac{\epsilon}{2}}$ . Specifically, given a expected number  $k$  of flipped bits and the length  $n$ , we can derive the probability according to the formula,  $Pr[H(\mathbf{h}', \mathbf{h}) = k] = \binom{n}{k} (\frac{1}{2}e^{-\frac{\epsilon}{2}})^k (1 - \frac{1}{2}e^{-\frac{\epsilon}{2}})^{(n-k)}$ ,

<sup>4</sup><https://pandas.pydata.org>

<sup>5</sup><https://scikit-learn.org/stable>



where  $H(\cdot)$  calculate the Hamming distance, and  $\mathbf{h}$  is perturbed code of  $\mathbf{h}$ . Then, when  $\epsilon = 1$ , take the case of 16 bits and  $k = 4$  for example, we can get the corresponding probability as approximately 20%. It means that when the code is longer, most valid bits can remain, and thus the performance can be maintained.

In summary, we suggest that it is unnecessary to integrate DP in *HashVFL* as it will decrease the performance. If DP is required, the length of the hash code needs to be expanded accordingly to maintain the performance.

TABLE XI  
PERFORMANCE COMPARISON WITH DIFFERENT PRIVACY BUDGETS. THE CELLS REPORT THE ACCURACY ON THE TEST SET.

Dataset	Code Length	$\epsilon = 1$	$\epsilon = 2$	$\epsilon = 10$	$\epsilon = \infty$
MNIST	4 Bits	34.28	61.73	97.26	<b>97.75</b>
	8 Bits	45.65	80.34	97.95	<b>98.34</b>
	16 Bits	65.62	93.35	98.21	<b>98.42</b>
CIFAR10	4 Bits	26.89	44.76	69.11	<b>70.83</b>
	8 Bits	33.54	57.40	72.99	<b>73.65</b>
	16 Bits	47.08	68.73	74.23	<b>74.96</b>
FER	4 Bits	27.57	39.08	50.57	<b>52.73</b>
	8 Bits	33.81	56.38	53.15	<b>54.50</b>
	16 Bits	40.32	51.56	<b>55.06</b>	55.00
CBPD	4 Bits	58.56	66.06	70.38	<b>70.98</b>
	8 Bits	61.99	67.85	75.68	<b>76.62</b>
	16 Bits	63.96	69.44	76.64	<b>77.35</b>
CRITEO	4 Bits	64.04	70.18	<b>73.82</b>	73.70
	8 Bits	64.55	71.03	72.74	<b>73.13</b>
	16 Bits	66.81	72.31	<b>74.03</b>	73.32
IMDb	4 Bits	64.03	68.51	<b>69.35</b>	68.59
	8 Bits	66.61	69.66	71.44	<b>72.10</b>
	16 Bits	68.26	70.21	72.42	<b>72.66</b>